PEPT2-CT was observed for PDZ2 and PDZ3, but not for PDZ1 and PDZ4 of PDZK1 (Figure 1c).

### *In vitro* binding of PEPT2 and PDZK1

We used a glutathione-*S*-transferase (GST) pull-down assay to confirm the ability of PEPT2-CT to bind to PDZK1 *in vitro* and validate the protein–protein interaction (Figure 2a). GST fusion proteins bearing the wild-type C-terminus (PEPT2-CT-wt) or C-terminal mutants (PEPT2-CTd3, L279A, and T727A) of PEPT2 were used to pull down *in vitro* translated full-length PDZK1. The data showed the same interaction specificity for PDZK1 and PEPT2 as exhibited in yeast two-hybrid assay (Figure 1a). As expected, the binding of PDZK1 to PEPT2 was completely abolished when the C-terminal PDZ motif was removed (PEPT2-CTd3) or mutated (PEPT2-CT-L729A or PEPT2-CT-T727A) (Figure 2a).

To confirm and quantify the interaction of PEPT2 with PDZK1, we performed surface plasmon resonance experiments using immobilized GST-PEPT2-CT and PDZ2 and PDZ3 of PDZK1 proteins independently fused to maltose-binding protein. As summarized in Table 1, the binding affinities of PDZ2 and PDZ3 of PDZK1 are low ($K_D = 10$ and 15 $\mu$M). These values are low in comparison to most PDZ domain interactions ($K_D = 1$ nM–10 $\mu$M).[39]

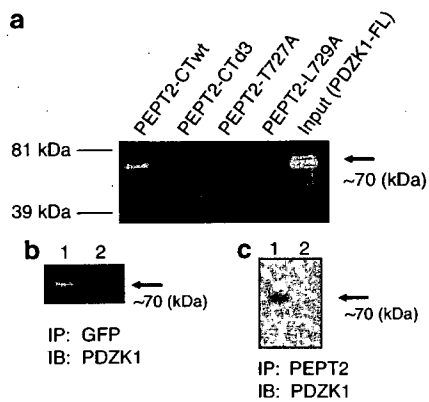


**Figure 2 | Interaction of PDZK1 with PEPT2.** (**a**) Full-length PDZK1 polymerase chain reaction product was *in vitro* translated in the presence of Transcend Biotinylated Lysine tRNA (Promega). The *in vitro* translation products were incubated with GST alone (lane 1), GST-PEPT2-CTwt (lane 2), or GST-PEPT2-CTd3 (lane 3) using a ProFound Pull-Down GST Protein:Protein Interaction kit (Pierce). The pull-down products were analyzed by sodium dodecyl sulfate-polyacrylamide gel electrophoresis. The input corresponds to the crude *in vitro* translation reaction. Positions of molecular mass standards are indicated on the right. GST fused to PEPT2 C-terminal wt can co-precipitate PDZK1, confirming the specificity found in the yeast two-hybrid system. The mutant form of PEPT2 in which the C-terminal PDZ recognition motif is removed is not able to precipitate PDZK1. (**b**) Co-immunoprecipitation of PEPT2 and PDZK1 in HEK293 cells. HEK293 cells were transfected with pEGFP-C2 vectors encoding PEPT2-wt (lane 1) or PEPT2-d3 (lane 2) with pcDNA3.1-PDZK1 and then immunoprecipitated with the anti-GFP antibody. Then, the immunoprecipitates were resolved by sodium dodecyl sulfate-polyacrylamide gel electrophoresis and probed with anti-PDZK1 antibodies. (**c**) Human kidney membrane fractions were immunoprecipitated with the anti-PEPT2 antibody (lane 1) and control immunoglobulin G (lane 2). The presence of PDZK1 in the immunoprecipitates was determined by Western blotting with the anti-PDZK1 antibody used in a previous study.[29]

### Co-immunoprecipitation from heterologous cells and tissue

To demonstrate that PEPT2 and PDZK1 can also interact in mammalian cells, we used a previously prepared rabbit polyclonal antibody against PDZK1.[29] We coexpressed full-length human PEPT2 fused with green fluorescent protein (GFP) (GFP-PEPT2) and PDZK1 in human embryonic kidney (HEK)293 cells. Wild-type GFP-PEPT2 was co-immunoprecipitated with a GFP-specific antibody but GFP-PEPT2 which lacked the last three residues was not precipitated with PDZK1 (Figure 2b).

Furthermore, we demonstrated an association between endogenous PDZK1 and PEPT2 in human tissue by co-immunoprecipitating PEPT2 from human kidney membrane fractions using the anti-PDZK1 antibody, but not control immunoglobulin G (Figure 2c). This result is the evidence that observed interaction occurs between protein partners expressed from endogenous genes in kidneys.

### Expression of PEPT2 in human kidney sections

In rats, Pept2 is present at the apical membrane of renal proximal tubules[14,15] and in humans, PDZK1 is reported to be expressed at the apical side of proximal tubular cells.[29,40] To determine whether PEPT2 and PDZK1 colocalize at the apical membrane of renal proximal tubules in humans, we carried out immunostaining of human serial kidney sections using anti-PEPT2 antibody.[41] Consistent with the previous reports, in the renal cortex, PEPT2 immunoreactivities were detected at the apical side of proximal tubular cells (Figure 3).

**Table 1 | Characteristics of interaction between PEPT2 C-terminus and PDZK1 PDZ domains 2 and 3 (PDZ2 and PDZ3)**

| Construct | $k_a$ (1/mM s) | $k_d$ (1/min) | $K_D$ ($\mu$M) |
|---|---|---|---|
| PDZK1-PDZ2 | $7.2 \times 10^2$ | $7.5 \times 10^{-3}$ | 10 |
| PDZK1-PDZ3 | $3.6 \times 10^2$ | $5.5 \times 10^{-3}$ | 15 |

The kinetic characteristics of the interaction with immobilized GST-fused PEPT2 C-terminus with the second and third PDZ domains of PDZK1 (PDZ2 and PDZ3) fused with MBP measured by SPR methods are summarized. Association rate constants ($k_a$), dissociation rate constants ($k_d$), and equilibrium dissociation constants ($K_D = k_d/k_a$) are given.

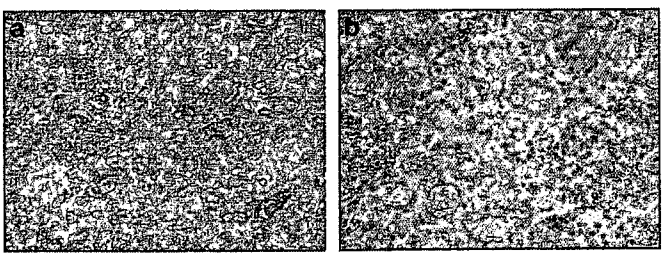


**Figure 3 | Immunohistochemical analysis of PEPT2 in human kidney sections.** (**a** and **b**) Immunohistochemical labeling of PEPT2 by diaminobenzidine reaction of human kidney. (**a**) PEPT2 was detected in proximal tubules in the cortex. (**b**) The apical membrane of proximal tubule was immunostained with the anti-hPET2 antibody and no immunostaining was observed in the basolateral membrane and glomeruli. These figures are representative of typical section samples. Original magnifications, (**a**) × 100 and (**b**) × 400.

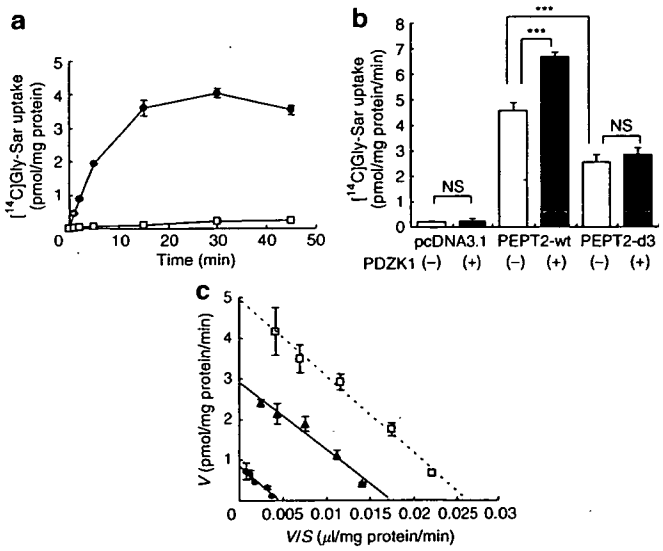


**Figure 4 | Effect of PDZK1 on PEPT2-mediated [$^{14}$C]Gly-Sar transport activity.** (**a**) The time profile of the uptake of [$^{14}$C]Gly-Sar via PEPT2. Intracellular accumulation of Gly-Sar was linear within 5 min and was significantly greater in PEPT2-wt-transfected HEK293 cells (HEK-PEPT2-wt; filled circles) than that in the mock-transfected cells (HEK-mock; open squares). (**b**) Coexpression of PEPT2 and PDZK1 increased [$^{14}$C]Gly-Sar uptake (30 $\mu$M) significantly over cells transfected with PEPT2 alone (closed column, middle). This effect was abolished when the C-terminal deletion mutant of PEPT2 was cotransfected with PDZK1 (HEK-PEPT2-d3; closed column, right), confirming that the interaction of PDZK1 with PEPT2 C-terminal domain is responsible for this effect. ***$P<0.001$ (**c**) Kinetic data using PEPT2-expressing HEK293 cells showed that PDZK1 (open squares) increased the $V_{max}$ from 2.92 to 4.95 fmol/mg protein/min and increased the $K_m$ slightly from 167 to 189 $\mu$M, as compared with PEPT2 alone (filled triangles). $V_{max}$ of [$^{14}$C]Gly-Sar transport via HEK-PEPT2-d3 decreased (0.86 pmol/mg protein/min), whereas its $K_m$ showed no change (187 nM) (filled circles). The kinetic parameters for the uptake via PEPT2 were estimated using $v = V_{max}[S]/(K_m + [S])$, where $v$ is the uptake rate of substrates, $[S]$ is the substrate concentration ($\mu$M) in the medium. $K_m$ is the Michaelis–Menten constant ($\mu$M) and $V_{max}$ is the maximum uptake rate (pmol/mg of protein/2 min). These parameters were determined using the Eadie–Hofstee equation.

### PEPT2 transport activity increases in presence of PDZK1

To determine whether PEPT2 and PDZK1 interaction is required to mediate the increase in PEPT2 transport activity, we transfected HEK293 cells with the pcDNA3.1(+) plasmid containing full-length PEPT2 (HEK-PEPT2-wt), PEPT2 lacking the last three amino acids (HEK-PEPT2-d3), or without an insert (HEK-mock). The time profile of the uptake of [$^{14}$C]glycylsarcosine (Gly-Sar) via PEPT2 is shown in Figure 4a. Intracellular accumulation of Gly-Sar was linear within 5 min and it was also significantly greater in HEK-PEPT2-wt than that in HEK-mock. After 2 min incubation, we demonstrated that [$^{14}$C]Gly-Sar uptake via HEK-PEPT2-wt was approximately 20-fold higher than that in HEK-mock and that in HEK-PEPT2-d3 was approximately 12-fold higher than that in HEK mock (Figure 4b). Gly-Sar transport activities significantly increased after PDZK1 coexpression (1.5-fold) (Figure 4b). This effect was not observed when PEPT2-d3 was coexpressed with PDZK1 (Figure 4b).

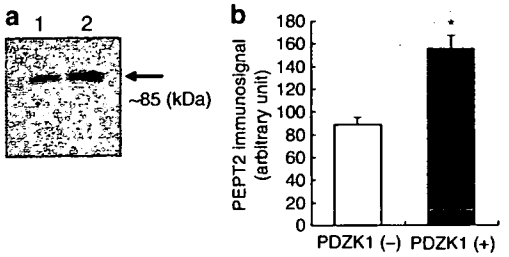


**Figure 5 | Surface expression level of PEPT2.** (**a**) cell surface biotinylation analysis of PEPT2 transiently expressing HEK293 cells transfected with vector alone (lane 1), and those transfected with PDZK1 (lane 2). Single bands of approximately 85 kDa, which are consistent with PEPT2, were observed in both lanes. (**b**) Quantification of immunosignal for PEPT2 ($n=3$, error bars are s.d.). Densitometric analysis was performed using Model DIANA II Imaging System (M&S Instruments Trading Inc., Tokyo, Japan). *$P<0.05$.

Next, we examined the effect of PDZK1 coexpression on the kinetics of [$^{14}$C]Gly-Sar transport via HEK-PEPT2-wt that had been transfected with pcDNA3.1-PDZK1 or pcDNA3.1 alone. Kinetic data showed that PDZK1 significantly increased $V_{max}$ from 2.92 to 4.95 pmol/mg protein/min and slightly increased $K_m$ from 167 to 189 nM, in comparison to PEPT2 alone (Figure 4c). Interestingly, the $V_{max}$ of [$^{14}$C]Gly-Sar transport via HEK-PEPT2-d3, decreased (0.86 pmol/mg protein/min), whereas its $K_m$ showed no change (187 nM).

### Surface expression level of PEPT2

To determine changes in the cell surface expression level of PEPT2, we used a cell-membrane-impermeant biotinylation reagent to selectively label the cell-surface proteins. After the treatment, the cell lysates from HEK293 cells transfected with PEPT2 and PDZK1 or PEPT2 and mock was collected. The amount of surface-biotinylated PEPT2 expression on plasma membranes increased 1.8-fold (PEPT2 and mock-transfected: $88.3 \pm 6.9$ vs PEPT2 and PDZK1-transfected: $155.5 \pm 11.3$ AU, $n=3$) when PDZK1 was coexpressed (Figure 5). This change seems close to the one in $V_{max}$ of PEPT2-mediated transport observed in Figure 4c.

## DISCUSSION

The proton-coupled peptide transporter PEPT2 (*SLC15A2*) mediates the high-affinity low-capacity transport of small peptides in the kidney. Therefore, PEPT2 is presumed to contribute to the conservation of peptide-bound amino acids. Although the transport properties and characteristics of substrate recognition for PEPT2 have been well documented, there is less information on PEPT2 regulation. A recent report by Kato *et al.*[31] has provided the novel idea concerning the modulation of PEPT2 function by its associated protein. They demonstrated an interaction between the recombinant PEPT2 C-terminus fused to GST and purified His-tagged PDZK1, but they solely rely on data from *in vitro* binding assays and did not indicate the physiological importance of this interaction. In addition, the yeast two-hybrid screens performed by Gisler *et al.*,[42] using baits

containing single PDZ domains derived from mouse PDZK1, failed to detect Pept2 as a candidate for PDZK1 binding although several membrane proteins including Urat1 were found. To identify PDZK1 as a physiological binding partner of PEPT2, we evaluated this interaction from several viewpoints in this study.

Starting from a yeast two-hybrid screening of a human kidney cDNA library, we have demonstrated PDZK1 to be a physiological interactor of PEPT2. First, we could detect PDZK1 from 64 positive clones by library screening. Second, we could observe the co-immunoprecipitation of PEPT2 and PDZK1 from kidney membrane fractions (Figure 2c). Third, we could demonstrate the localization of PEPT2 protein at the apical side of the renal proximal tubules where PDZK1 is also expressed (Figure 3). These results indicate the physiological meaning of this interaction.

We have further examined this interaction by a yeast two-hybrid assay (Figure 1), an *in vitro* pull-down assay (Figure 2a), co-immunoprecipitation (Figure 2b) and surface plasmon resonance assay (Table 1) of recombinant proteins, as well as by the transport studies (Figure 4) and a cell surface biotinylation assay (Figure 5). These results support the preliminary data presented by Kato *et al.*[31] Moreover, the augmentation of the transport activity by PDZK1 was accompanied by a significant increase in the $V_{max}$ of Gly-Sar transport via PEPT2 (Figure 4c) and was associated with the increased surface expression level of PEPT2 in HEK293 cells (Figure 5). These characteristics are closely similar to those of the URAT1–PDZK1 interaction,[29] and suggest PDZK1 to thus play a similar role in PEPT2–PDZK1 interaction; namely, that PEPT2 is stabilized and/or anchored at the cell membrane, making it less likely to be internalized and subsequently degraded.

Although their functional consequences are the same, there are several differences between the PEPT2–PDZK1 interaction and the URAT1–PDZK1 interaction. First, the frequency of PDZK1 appearing as a positive clones was smaller in the case of PEPT2 (one out of 64) than in the case of URAT1 (35 out of 98). Second, the interaction profiles of PDZK1 ligand against individual PDZ domains of PDZK1 were different, although they have similar C-terminal PDZ motifs: T-K-L for PEPT2 and T-Q-F for URAT1. PEPT2 binds to PDZ2 and PDZ3 (Figure 1), while URAT1 binds to PDZ1, PDZ2, and PDZ4.[29] Third, the binding affinities for each PDZ domain of PDZK1 were more than 10-fold lower for PEPT2 than for URAT1: 10 and 15 $\mu$M for PEPT2 (Table 1) and 1.97–514 nM for URAT1.[29] Fourth, when a C-terminal deletion mutant of URAT1 (URAT1-d3) was coexpressed with PDZK1, urate transport activity was not enhanced, but URAT1-d3 still demonstrated a similar urate transport activity to wt URAT1 when expressed without PDZK1. In contrast, the C-terminal deletion mutant of PEPT2 (PEPT2-d3) not only lacked the ability to enhance transport activity when coexpressed with PDZK1, but its transport activity was reduced to half that of the wt PEPT2 (PEPT2-wt) when expressed without PDZK1.

The low frequency of PDZK1 in PEPT2 screening seems consistent with the report of Gisler *et al.*[42] as we mentioned earlier in this paper. In addition to the expression levels of these proteins, the binding affinity is likely to affect the frequency of a particular protein appearing as a positive clone in yeast two-hybrid screening. Therefore, a low frequency of positive clone does not mean that the observed interaction is physiologically less important. Moreover, a low binding affinity may be advantageous for the regulatory dynamics of protein–protein interactions,[27] because a low binding affinity is related to an easier association and dissociation of proteins than a high binding affinity. In particular, PEPT2 has a putative protein kinase C (PKC) recognition site at its C-terminal close to the PDZ motif, whose phosphorylation may interfere with binding to the PDZ domain.[43] It will be interesting to investigate whether the phosphorylation of both PEPT2 and PDZK1 or either protein independently alters the binding affinity of this interaction, in order to clarify the regulatory mechanism for PDZ–ligand interaction.

The decreased transport activity of the PEPT2 C-terminal deletion mutant compared to wt PEPT2, together with the significant reduction in $V_{max}$ (Figure 4) may indicate PDZ motif to thus play another role in the PEPT2-CT: the targeting of the transporter to the plasma membrane. This was originally predicted by Russel *et al.*[28] However, as mentioned above, this phenomenon was not observed in the C-terminal deletion mutant of URAT1 expressed in the same HEK293 cells that have endogenous PDZK1 at low level.[29] Although we frequently detected PDZK1 in the URAT1 screen, we did not find any other binding candidates for URAT1. In the PEPT2 screen, we detected several potential binding partners for PEPT2 besides PDZK1 (manuscript in preparation). It will therefore be important to identify other binding proteins surrounding PEPT2 to understand the potential significance of this interaction.

Recently, PDZ proteins have been recognized as orchestrating scaffolds to achieve concerted functions.[23] PEPT2 mediates an electrogenic proton-coupled cotransport that uses an inward proton gradient to transport small peptides from urine to the cell. Following the concept proposed by Moe, the ability of PDZK1 to couple PEPT2 to the $Na^+/H^+$ exchanger NHE3 may provide the necessary lumen-to-cell proton gradient, and the multimolecular protein complex will be functionally equivalent to a $Na^+$/oligopeptide cotransporter. A functional coupling between PEPT2 and NHE1 and/or NHE2 has recently been shown by Wada *et al.*[44] In this paper, we described, for the first time, the exact localization of PEPT2 in the human kidney in addition to its novel regulatory mechanism. PEPT2 proteins are expressed at the apical membrane of renal proximal tubules similarly to rat Pept1 and rat Pept2, which are expressed in the same site.[15] Based on the above findings, human PEPT2 may therefore be involved in the reabsorption of peptides on the apical side of the renal tubules, similar to that of rodent Pept2 and the protein complex surrounding PEPT2 should thus be clarified by identifying other interacting proteins to obtain a

**Table 2 | PCR primers used in this study**

| Construct | Sense primer | Antisense primer |
|---|---|---|
| PEPT2-CTwt | 5′-CGAATTCCTGCCCGAGACCCAGAG-3′ | 5′-CTCTCGAGCTAAAACTGTGTGGATTTTA-3′ |
| PEPT2-CTd3 | 5′-CGAATTCCTGCCCGAGACCCAGAG-3′ | 5′-CCCTCGAGCTAGGATTTTAGGACAGAGTTC-3′ |
| PEPT2-L727A | 5′-CGAATTCCTGCCCGAGACCCAGAG-3′ | 5′-CCCTCGAGCTAAGCCTGTGTGGATTTTAGGA-3′ |
| PEPT2-T729A | 5′-CGAATTCCTGCCCGAGACCCAGAG-3′ | 5′-CCCTCGAGCTAAAACTGTGCGGATTTTA-3′ |

PCR, polymerase chain reaction; wt, wild type.

comprehensive understanding of the peptide transport function in the renal proximal tubules.

## MATERIALS AND METHODS

### Materials

[$^{14}$C]Glycosylsarcosine (Gly-Sar) (4 Ci/mmol) was obtained from Moravek (Brea, CA, USA). Other materials used included Ham F12 medium from Nissui Pharmaceutical Co., Ltd. (Tokyo, Japan), and fetal bovine serum and trypsin from Invitrogen (Carlsbad, CA, USA).

### Cloning of human PEPT2 cDNA

The cDNA library was prepared from human kidney poly(-A)$^+$RNA.[45] The 0.46-kb cDNA fragment (24–481 nt of the nucleotide sequence of human PEPT2 (hPEPT2)) was obtained by polymerase chain reaction. This fragment was labeled with [$^{32}$P]dCTP (T7QuickPrime, Amersham Biosciences, Tokyo, Japan) and used as probe. The screening of the cDNA library was performed as described elsewhere.[46]

### Plasmid construction

The C-terminal fragments of wt hPEPT2 cDNA and three mutants (designated d3, L729A, and T727A) were generated by polymerase chain reaction using specific primers (Table 2) and cloned into the *Bam*HI and *Xho*I sites of pEG202 (bait) and pGEX-6P-1 (Amersham Biosciences) to construct PEPT2-CTwt, PEPT2-CTd3, PEPT2-L729A, and PEPT2-T727A. The full-length coding sequences of hPEPT2 (wt) as well as its C-terminal 3-amino-acid-deletion mutant (d3) were inserted into the mammalian expression vector pcDNA3.1 (Invitrogen) for functional analysis and into pEGFP-C2 (Clontech, Tokyo, Japan) for GFP fusion protein preparation. The pcDNA3.1 vector containing the full-length human PDZK1 (hPDZK1) and preys (pJG4–5 and pMAL-C2x) containing single PDZ domains of hPDZK1 were prepared as described previously.[29]

### Yeast two-hybrid assay

A human kidney cDNA library was constructed as described previously.[29] A PEPT2 C-terminal bait corresponding to the last 34 amino acids of PEPT2 was used to screen $8.7 \times 10^6$ clones of the human kidney cDNA library with the LexA-based GFP two-hybrid system (Grow'n' Glow system; MoBiTec, Göttingen, Germany).

### *In vitro* binding assay

PEPT2-CT for GST fusion protein production in bacteria as reported previously.[47] *In vitro* translation was performed from a plasmid carrying the full-length PDZK1 with the TNT T7 Quick for polymerase chain reaction DNA system (Promega, Tokyo, Japan) in the presence of Transcend Biotinylated tRNA (Promega), as described elsewhere.[29] Of *in vitro*-translated products, (5 μl) was applied into ProFound™ Pull-Down GST Protein:Protein Interaction Kit (Pierce, Rockford, IL, USA) with 50 μl of GST-glutathione-Sepharose resin and protein complexes were eluted according to the manufacturer's instructions.

### Surface plasmon resonance

The interactions of PEPT2-CT with the second and third PDZ domains of PDZK1 were investigated using a BIAcore 3000 analytical system (BIAcore AB, Tokyo, Japan). Using an amine coupling kit, GST-fused wt PEPT2-CT or GST alone was attached to a CM5 sensor chip according to the manufacturer's instructions, giving an increase of 11 214 resonance units (RU) for GST-PEPT2-CT or 8,566 resonance units for GST alone. Binding experiments were performed with the PDZK1 single PDZ domains fused with maltose-binding protein as described elsewhere.[29]

### Immunohistochemical analysis

We used human single-tissue slides (Biochain, Hayward, CA, USA) for light microscopic immunohistochemical analysis as reported previously.[48] They were treated with 10 μg/ml primary rabbit polyclonal antibodies against PEPT2[41] or PDZK1 (4°C overnight).

### Cell culture and transfection

HEK293 cells were maintained in Dulbecco's-modified Eagle's medium supplemented with 10% fetal bovine serum, 1 mM sodium pyruvate, penicillin (100 U/ml), and streptomycin (100 mg/ml) (Invitrogen) at 37°C in 5% $CO_2$. Transient transfection with Lipofectamine 2000 (Invitrogen, Gaithersburg, MD, USA) was performed according to the manufacturer's recommendations.

### Immunoprecipitation and immunoblotting

Immunoprecipitation analysis was performed as described previously.[49] Lysates from HEK293 cells that expressed GFP-fused hPEPT2 and hPDZK1 were immunoprecipitated by the anti-GFP antibody (full-length A.v. polyclonal antibody, Clontech). For the co-immunoprecipitation of endogenous PEPT2 and PDZK1, we used human kidney membrane fractions (Biochain) and added the anti-PEPT2 antibody or control immunoglobulin G to this solution. After overnight incubation, PEPT2 and PDZK1 were immunoprecipitated using the Seize Classic (A) Immunoprecipitation kit (Pierce). The affinity-purified rabbit PDZK1 antibody and horseradish peroxidase-conjugated goat anti-rabbit immunoglobulin G (Amersham Biosciences) were used for immunoblotting with enhanced chemiluminescence reagents (ECL Plus, Amersham Biosciences).

### Gly-Sar transport activity assay

HEK293 cells were plated on 24-well culture plates at a density of $2 \times 10^5$ cells/well 24 h prior to transfection, and they were transfected as described above. After 36 h, the culture medium was removed, and the cells were washed three times and incubated in

serum-free Hank's solution (containing in mM: 125 NaCl, 5.6 glucose, 4.8 KCl, 1. 2 $MgSO_4 \cdot 7H_2O$, 1.2 $KH_2PO_4$, 1.3 $CaCl_2 \cdot 2H_2O$, 25 *N*-2-hydroxyethylpiperazine-*N'*-2-ethanesulfonic acid (pH 6.0)) for 10 min. The uptake study was started by adding 500 $\mu$l of solution containing 30 $\mu$M [$^{14}$C]Gly-Sar to the plate. After 2 min, the cells were washed twice in an ice-cold solution, and lysed in 0.1 N NaOH for 20 min for scintillation counting.

To determine the kinetic parameters, the concentrations of Gly-Sar were varied from 30 to 1000 $\mu$M. PEPT2-mediated Gly-Sar uptake was calculated as the difference between the uptake rates into HEK293 cells transiently expressing PEPT2 and those into HEK293 cells transfected with the vector (pcDNA3.1, Invitrogen) only.

### Cell surface biotinylation

Surface biotinylation of PEPT2 at the plasma membrane was performed as described elsewhere.[49] Surface proteins in HEK293 cells transfected with pcDNA3.1(+)-hPEPT2 and pcDNA3.1(+)-hPDZK1 or pcDNA3.1(+) empty vector (mock) were biotinylated with Sulfo-NHS-SS-Biotin (Pierce) (0.5 mg/ml) in phosphate-buffered saline for 30 min at 4°C. Cell lysates were then incubated with Ultralink-immobilized NeutrAvidin beads (Pierce) to precipitate biotinylated proteins. PEPT2 was detected with polyclonal PEPT2 antibody (1:10,000).[41]

### Statistical analysis

Uptake experiments were conducted three times, and each uptake experiment was performed in triplicate. Values are presented as the mean $\pm$ s.e. Statistical significance was determined by Student's *t*-test.

#### ACKNOWLEDGMENTS

We thank Akie Toki and Keiko Sakama for technical assistance. The anti-hPDZK1 polyclonal antibody was supplied by Transgenic Inc., Kumamoto, Japan. This work was supported in part by grants from the Ministry of Education, Culture, Sports, Science and Technology of Japan, the Japan Society for the Promotion of Science, Research on Health Sciences focusing on Drug Innovation from the Japan Health Sciences Foundation, Mutual Aid Corporation for Private Schools of Japan, the Nakatomi Foundation, the Salt Science Research Foundation (No. 0524), the Japan Foundation of Applied Enzymology, Astellas Foundation for Research on Metabolic Disorders, Gout Research Foundation of Japan, Heiwa Nakajima Foundation, and Health and Labor Sciences Research Grants for Research on Advanced Medical Technology: Toxicogenomics Project. This work was presented in part at the Annual Meeting of Experimental Biology 2004, Washington DC, April 2004, and published in abstract form (*FASEB J* **18**:A695, 2004).

#### REFERENCES

1. Daniel H, Rubio-Aliaga I. An update on renal peptide transporters. *Am J Physiol Renal Physiol* 2003; **284**: F885–F892.
2. Nielsen CU, Brodin B. Di/tri-peptide transporters as drug delivery targets: regulation of transport under physiological and patho-physiological conditions. *Curr Drug Targets* 2003; **4**: 373–388.
3. Terada T, Inui K. Peptide transporters: structure, function, regulation and application for drug delivery. *Curr Drug Metab* 2004; **5**: 85–94.
4. Boll M, Markovich D, Weber WM *et al.* Expression cloning of a cDNA from rabbit small intestine related to proton-coupled transport of peptides, lactam antibiotics and ACE-inhibitors. *Pflugers Arch* 1994; **429**: 146–149.
5. Fei YJ, Kanai Y, Nussberger S *et al.* Expression cloning of a mammalian proton-coupled oligopeptide transporter. *Nature* 1994; **368**: 563–566.
6. Boll M, Herget M, Wagener M *et al.* Expression cloning and functional characterization of the kidney cortex high-affinity proton-coupled peptide transporter. *Proc Natl Acad Sci USA* 1996; **93**: 284–289.
7. Saito H, Okuda M, Terada T *et al.* Cloning and characterization of a rat H+/peptide cotransporter mediating absorption of $\beta$-lactam antibiotics in the intestine and kidney. *J Pharmacol Exp Ther* 1995; **275**: 1631–1637.
8. Miyamoto KI, Shiraga T, Morita K *et al.* Sequence, tissue distribution and developmental changes in rat intestinal oligopeptide transporter. *Biochim Biophys Acta* 1996; **1305**: 34–38.
9. Saito H, Terada T, Okuda M *et al.* Molecular cloning and tissue distribution of rat peptide transporter PEPT2. *Biochim Biophys Acta* 1996; **1280**: 173–177.
10. Liang R, Fei YJ, Prasad PD *et al.* Human intestinal $H^+$/peptide cotransporter. Cloning, functional expression, and chromosomal localization. *J Biol Chem* 1995; **270**: 6456–6463.
11. Liu W, Liang R, Ramamoorthy S *et al.* Molecular cloning of PEPT2, a new member of the $H^+$/peptide cotransporter family, from human kidney. *Biochim Biophys Acta* 1995; **1235**: 461–466.
12. Ramamoorthy S, Liu W, Ma YY *et al.* Proton/peptide cotransporter (PEPT2) from human kidney: functional characterization and chromosomal localization. *Biochim Biophys Acta* 1995; **1240**: 1–4.
13. Smith DE, Pavlova A, Berger UV *et al.* Tubular localization and tissue distribution of peptide transporters in rat kidney. *Pharm Res* 1998; **15**: 1244–1249.
14. Ogihara H, Saito H, Shin BC *et al.* Immuno-localization of $H^+$/peptide cotransporter in rat digestive tract. *Biochem Biophys Res Commun* 1996; **220**: 848–852.
15. Shen H, Smith DE, Yang T *et al.* Localization of PEPT1 and PEPT2 proton-coupled oligopeptide transporter mRNA and protein in rat kidney. *Am J Physiol* 1999; **276**: F658–F665.
16. Rubio-Aliaga I, Frey I, Boll M *et al.* Targeted disruption of the peptide transporter Pept2 gene in mice defines its physiological role in the kidney. *Mol Cell Biol* 2003; **23**: 3247–3252.
17. Takahashi K, Masuda S, Nakamura N *et al.* Upregulation of H(+)-peptide cotransporter PEPT2 in rat remnant kidney. *Am J Physiol Renal Physiol* 2001; **281**: F1109–F1116.
18. Nakamura N, Masuda S, Takahashi K *et al.* Decreased expression of glucose and peptide transporters in rat remnant kidney. *Drug Metab Pharmacokinet* 2004; **19**: 41–47.
19. Wenzel U, Diehl D, Herget M *et al.* Regulation of the high-affinity H+/peptide cotransporter in renal LLC-PK1 cells. *J Cell Physiol* 1999; **178**: 341–348.
20. Bravo SA, Nielsen CU, Amstrup J *et al.* Epidermal growth factor decreases PEPT2 transport capacity and expression in the rat kidney proximal tubule cell line SKPT0193 cl.2. *Am J Physiol Renal Physiol* 2004; **286**: F385–F393.
21. Biber J. Emerging roles of transporter-PDZ complexes in renal proximal tubular reabsorption. *Pflugers Arch* 2001; **443**: 3–5.
22. Levi M. Role of PDZ domain-containing proteins and ERM proteins in regulation of renal function and dysfunction. *J Am Soc Nephrol* 2003; **14**: 1949–1951.
23. Moe OW. Scaffolds: orchestrating proteins to achieve concerted function. *Kidney Int* 2003; **64**: 1916–1917.
24. Anzai N, Jutabha P, Kanai Y, Endou H. Integrated physiology of proximal tubular organic anion transport. *Curr Opin Nephrol Hypertens* 2005; **14**: 472–479.
25. Fanning AS, Anderson JM. Protein modules as organizers of membrane structure. *Curr Opin Cell Biol* 1999; **11**: 432–439.
26. Garner CC, Nash J, Huganir RL. PDZ domains in synapse assembly and signalling. *Trends Cell Biol* 2000; **10**: 274–280.
27. Hung AY, Sheng M. PDZ domains: structural modules for protein complex assembly. *J Biol Chem* 2002; **277**: 5699–5702.
28. Russel FGM, Masereeuw R, van Aubel RAMH. Molecular aspects of renal anionic drug transport. *Annu Rev Physiol* 2002; **64**: 563–594.
29. Anzai N, Miyazaki H, Noshiro R *et al.* The multivalent PDZ domain-containing protein PDZK1 regulates transport activity of renal urate-anion exchanger URAT1 via its C-terminal. *J Biol Chem* 2004; **279**: 45942–45950.
30. Anzai N, Enomoto A, Endou H. Renal urate handling: clinical relevance of recent advances. *Curr Rheumatol Rep* 2005; **7**: 227–234.
31. Kato Y, Yoshida K, Watanabe C *et al.* Screening of the interaction between xenobiotic transporters and PDZ proteins. *Pharm Res* 2004; **21**: 1886–1894.
32. Kocher O, Comella N, Tognazzi K, Brown LF. Identification and partial characterization of PDZK1: a novel protein containing PDZ interaction domains. *Lab Invest* 1998; **78**: 117–125.
33. Hernando N, Wagner CA, Gisler SM *et al.* PDZ proteins and proximal ion transport. *Curr Opin Nephrol Hypertens* 2004; **13**: 569–574.

34. Weinman EJ, Steplock D, Wang Y, Shenolikar S. Characterization of a protein cofactor that mediates protein kinase A regulation of the renal brush border membrane $Na^+$-$H^+$ exchanger. *J Clin Invest* 1995; **95**: 2143–2149.
35. Reczek D, Berryman M, Bretscher J. Identification of EBP50: a PDZ-containing phosphoprotein that associates with members of the ezrin-radixin-moesin family. *J Cell Biol* 1997; **139**: 169–179.
36. Hall RA, Ostedgaard LS, Premont RT *et al.* A C-terminal motif found in the beta2-adrenergic receptor, P2Y1 receptor and cystic fibrosis transmembrane conductance regulator determines binding to the $Na^+/H^+$ exchanger regulatory factor family of PDZ proteins. *Proc Natl Acad Sci USA* 1998; **95**: 8496–8501.
37. Scott RO, Thelin WR, Milgram SL. A novel PDZ protein regulates the activity of guanylyl cyclase C, the heat-stable enterotoxin receptor. *J Biol Chem* 2002; **277**: 22934–22941.
38. Songyang Z, Fanning AS, Fu C *et al.* Recognition of unique carboxyl-terminal motifs by distinct PDZ domains. *Science* 1997; **275**: 73–77.
39. Harris BZ, Lim WA. Mechanism and role of PDZ domains in signaling complex assembly. *J Cell Sci* 2001; **114**: 3219–3231.
40. Kocher O, Comella N, Gilchrist A *et al.* PDZK1, a novel PDZ domain-containing protein up-regulated in carcinomas and mapped to chromosome 1q21, interacts with cMOAT (MRP2), the multidrug resistance-associated protein. *Lab Invest* 1999; **79**: 1161–1170.
41. Terada T, Irie M, Okuda M, Inui K. Genetic variant Arg57His in human $H^+$/peptide cotransporter 2 causes a complete loss of transport function. *Biochem Biophys Res Commun* 2004; **316**: 416–420.
42. Gisler SM, Pribanic S, Bacic D *et al.* PDZK1: I. A major scaffolder in brush borders of proximal tubular cells. *Kidney Int* 2003; **64**: 1733–1745.
43. Daniel H, Herget M. Cellular and molecular mechanisms of renal peptide transport. *Am J Physiol* 1997; **273**: F1–F8.
44. Wada M, Miyakawa S, Shimada A *et al.* Functional linkage of $H^+$/peptide transporter PEPT2 and $Na^+/H^+$ exchanger in primary cultures of astrocytes from mouse cerebral cortex. *Brain Res* 2005; **1044**: 33–41.
45. Cha SH, Sekine T, Fukushima J *et al.* Identification and characterization of human organic anion transporter 3 expressing predominantly in the kidney. *Mol Pharmacol* 2001; **59**: 1277–1286.
46. Sakata T, Anzai N, Shin HJ *et al.* Novel single nucleotide polymorphisms of organic cation transporter 1 (*SLC22A1*) affecting transport functions. *Biochem Biophys Res Commun* 2004; **313**: 789–793.
47. Anzai N, Deval E, Schaefer L *et al.* The multivalent PDZ domain-containing protein CIPP is a partner of acid-sensing ion channel 3 in sensory neurons. *J Biol Chem* 2002; **277**: 16655–16661.
48. Ekaratanawong S, Anzai N, Jutabha P *et al.* Human organic anion transporter 4 is a renal apical organic anion/dicarboxylate exchanger in the proximal tubules. *J Pharmacol Sci* 2004; **94**: 297–304.
49. Miyazaki H, Anzai N, Ekaratanawong S *et al.* Modulation of renal apical organic anion transporter 4 (OAT4) function by two PDZ domain-containing proteins. *J Am Soc Nephrol* 2005; **16**: 3498–3506.

# Identification and Functional Characterization of a New Human Kidney–Specific $H^+$/Organic Cation Antiporter, Kidney-Specific Multidrug and Toxin Extrusion 2

Satohiro Masuda,* Tomohiro Terada,* Atsushi Yonezawa,* Yuko Tanihara,* Koshiro Kishimoto,* Toshiya Katsura,* Osamu Ogawa,† and Ken-ichi Inui*

**Department of Pharmacy, Kyoto University Hospital, Faculty of Medicine, and †Department of Urology, Graduate School of Medicine, Kyoto University, Kyoto, Japan*

**A cDNA coding a new $H^+$/organic cation antiporter, human kidney-specific multidrug and toxin extrusion 2 (hMATE2-K), has been isolated from the human kidney. The hMATE2-K cDNA had an open reading frame that encodes a 566–amino acid protein, which shows 94, 82, 52, and 52% identity with the hMATE2, hMATE2-B, hMATE1, and rat MATE1, respectively. Reverse transcriptase–PCR revealed that hMATE2-K mRNA but not hMATE2 was expressed predominantly in the kidney, and hMATE2-B was ubiquitously found in all tissues examined except the kidney. The immunohistochemical analyses revealed that the hMATE2-K as well as the hMATE1 was localized at the brush border membranes of the proximal tubules. HEK293 cells that were transiently transfected with the hMATE2-K cDNA but not hMATE2-B exhibited the $H^+$ gradient–dependent antiport of tetraethylammonium (TEA). Transfection of hMATE2-B had no affect on the hMATE2-K–mediated transport of TEA. hMATE2-K also transported cimetidine, 1-methyl-4-phenylpyridinium (MPP), procainamide, metformin, and $N^1$-methylnicotinamide. Kinetic analyses demonstrated that the Michaelis-Menten constants for the hMATE2-K–mediated transport of TEA, MPP, cimetidine, metformin, and procainamide were 0.83 mM, 93.5 μM, 0.37 mM, 1.05 mM, and 4.10 mM, respectively. Ammonium chloride–induced intracellular acidification significantly stimulated the hMATE2-K–dependent transport of organic cations such as TEA, MPP, procainamide, metformin, $N^1$-methylnicotinamide, creatinine, guanidine, quinidine, quinine, thiamine, and verapamil. These results indicate that hMATE2-K is a new human kidney–specific $H^+$/organic cation antiporter that is responsible for the tubular secretion of cationic drugs across the brush border membranes.**

*J Am Soc Nephrol* 17: 2127–2135, 2006. doi: 10.1681/ASN.2006030205

Vectorial secretion of cationic compounds across the tubular epithelial cells is an important function of the kidney. Using the stopped flow tubular microperfusion method, cultured renal epithelial cells, and isolated membrane vesicles, it was suggested that two functionally distinct organic cation transporters were expressed in the basolateral and brush border membranes, respectively (1,2). Organic cations are suggested to accumulate in the renal tubular cells *via* a basolateral organic cation transport system that is sensitive to membrane potential differences. The intracellular cationic compounds were secreted by the apical $H^+$/organic cation antiport system, which was driven by an oppositely directed $H^+$ gradient. A prototype substrate, tetraethylammonium (TEA), has been used consistently for the functional characterization of these organic cation transport systems in the kidney (3–7).

Since cloning of the organic cation transporter OCT1 from the rat kidney (8), many related transporter proteins have been cloned and characterized. It is widely known that the basolateral entry of cationic compounds is mediated mainly by hepatic hOCT1 (SLC22A1) and renal hOCT2 (SLC22A2) in humans, depending on the membrane potential (9–11). However, attempts at molecular identification of the apical $H^+$/organic cation antiporter have failed for more than a decade. Recently, *in silico* homology screening of the human cDNA database identified a $H^+$/organic cation antiporter, human multidrug and toxin extrusion 1 (hMATE1), from the human brain using the NorM $Na^+$/multidrug antiporter in *Vibrio parahaemolyticus* as a reference (12). hMATE1 was expressed in the liver, kidney, and skeletal muscle and weakly in the brain and the heart. Although an isoform of hMATE1, hMATE2, was reported simultaneously to be expressed primarily in the kidney, the functional characteristics of hMATE2 were not examined.

In this study, we cloned hMATE2 cDNA from the human kidney for functional characterization. Sequence analysis revealed that the newly cloned cDNA was an alternative splice variant of hMATE2. It is interesting that real-time PCR and reverse transcriptase–PCR (RT-PCR) analyses clearly indicated that the newly cloned hMATE2 but not the original hMATE2 was expressed only in the kidney, showing a function of oppositely directed $H^+$ gradient–dependent antiport of organic

*Received March 7, 2006. Accepted May 15, 2006.*

*Published online ahead of print. Publication date available at www.jasn.org.*

**Address correspondence to:** Prof. Ken-ichi Inui, Department of Pharmacy, Kyoto University Hospital, Faculty of Medicine, Kyoto University, Sakyo-ku, Kyoto 606-8507, Japan. Phone: +81-75-751-3577; Fax: +81-75-751-4207; E-mail: inui@kuhp.kyoto-u.ac.jp



ISSN: 1046-6673/1708-2127

cations; therefore, we designated the new clone human kidney-specific multidrug and toxin extrusion (hMATE2-K).

## Materials and Methods

[$^{14}$C]TEA (2.035 GBq/mmol), [$^{14}$C]creatinine (2.035 GBq/mmol), [$^{14}$C]procainamide (2.035 GBq/mmol), [methyl-$^{14}$C]choline (2.035 GBq/mmol), [9-$^{3}$H]quinidine (740 GBq/mmol), [$^{3}$H]quinine (740 GBq/mmol), [$^{3}$H (G)]thiamine (370 GBq/mmol), L-[N-methyl-$^{3}$H]carnitine (3.145 TBq/mmol), [N-methyl-$^{14}$C]nicotine (2.035 TBq/mmol), [N-methyl-$^{3}$H]verapamil (2.96 TBq/mmol), and [7-$^{3}$H (N)]tetracycline (185 GBq/mmol) were obtained from American Radiolabeled Chemicals Inc. (St. Louis, MO). [$^{14}$C]Metformin (962 MBq/mmol) and [$^{14}$C]guanidine hydrochloride (1.961 GBq/mmol) were purchased from Moravek Biochemicals Inc. (Brea, CA). [$^{3}$H]1-Methyl-4-phenylpyridinium acetate (MPP; 2.7 TBq/mmol), [$^{14}$C]*p*-aminohippuric acid (1.9 GBq/mmol), and [$^{3}$H]glycylsarcosine (148 GBq/mmol) were from PerkinElmer Life Analytical Sciences (Boston, MA). [*N*-Methyl-$^{3}$H]Cimetidine (451 GBq/mmol) was from Amersham Biosciences (Uppsala, Sweden). [$^{14}$C]Levofloxacin (1.07 GBq/mmol) was from Daiichi Pharmaceutical Co., Ltd. (Tokyo, Japan). $N^1$-Methylnicotinamide (NMN) was obtained from Sigma (St. Louis, MO). [$^{14}$C]Captopril (0.115 GBq/mmol; Sankyo Co., Tokyo, Japan), cephalexin (Shionogi, Osaka, Japan), cefazolin (Astellas Pharma Inc., Tokyo, Japan), and cephradine (Sankyo Co.) were gifts from the respective suppliers. All other chemicals used were of the highest purity available.

### *Isolation of hMATE2-K cDNA*

The hMATE2 cDNA was cloned by RT-PCR from Marathon-Ready human kidney cDNA (Clontech, Palo Alto, CA). Primers that are specific for hMATE2 were designed on the basis of the sequence information of FLJ31196 (NM_152908). The forward and reverse primers, with mutations creating restriction enzyme sites (italics) for cloning the hMATE2 cDNA, were 5′-AGGGTACCCAGTGCCCCGGCCAGGAATGGA-3′ and 5′-CTGT*CTAGA*CCCCTCTGAGTGTCACCACAA-3′, respectively. Simultaneously, hMATE2 cDNA was cloned using the Marathon-Ready human brain cDNA (Clontech) as above. The PCR product was subcloned into the expression vector pcDNA3.1 (+) (Invitrogen, Carlsbad, CA) and sequenced using a multicapillary DNA sequencer RISA384 system (Shimadzu, Kyoto, Japan). Because both hMATE2 from the human kidney and brain were suggested to be splice variants of hMATE2 (FLJ31196) (12), we redesignated newly isolated clones from the human kidney and the human brain as hMATE2-K and hMATE2-B, respectively (Figure 1). The nucleotide sequences of hMATE2-K and hMATE2-B have been submitted to the DDBJ/EMBL/GenBank Data Bank as accession nos. AB250364 and AB250701, respectively.

### *Real-Time PCR and RT-PCR*

Total RNA from various human tissues was purchased from BioChain (Hayward, CA). RT of the total RNA (500 ng/20 μl reaction) and real-time PCR were carried out as described previously (13). The primer-probe sets used for hMATE1 and hMATE2 are summarized in Table 1. Glyceraldehyde-3-phosphate dehydrogenase (GAPDH) mRNA was checked for the quality of the total RNA of human tissues used with GAPDH Control Reagent (Applied Biosystems). To detect independently both hMATE2-K and hMATE2 mRNA, we designed qualitative PCR primers as summarized in Table 1.

### *Polyclonal Antibodies and Immunohistochemical Analyses*

Polyclonal antibodies were raised against the synthetic peptide that corresponded to the intracellular domains of hMATE1 (CQQAQVHANLKVN, no. 466-478) or hMATE2-K (YSRSECHVDFFRTPEE, no. 543-558) as described, respectively (14,15). For immunofluorescence histochemistry, the human renal specimens were fixed with 4% paraformaldehyde in PBS at 4°C for 30 min (13). Fixed tissues were embedded in OCT compound (Sakura Finetechnical, Tokyo, Japan) and frozen rapidly in liquid nitrogen. Sections (6 μm thick) were cut and covered with 2% FBS and 1 mg/ml RNase A (Nacalai Tesque, Kyoto, Japan) for 1 h. The covered sections were incubated for 1 h with antiserum (1:100 dilution) specific for hMATE1, hMATE2-K, hOCT2, a control of basolateral transporter, or hOCTN2, a control of luminal transporter, and then incubated with Cy3-labeled donkey anti-rabbit IgG (CALTAG Laboratory, San Francisco, CA), 5 U/ml Alexa 488-phalloidin (Molecular Probe, Eugene, OR), and 4′,6-diamidino-2-phenylindole for 1 h. These sections were examined with a BX-50-FLA fluorescence microscope (Olympus, Tokyo, Japan) at ×100 magnification. Images were captured with a DP-50 CCD camera (Olympus) using Studio Lite software (Olympus). As controls, specific rabbit antibodies were replaced with preimmune rabbit serum.

```
hMATE2-K  532 ------------------------------------------------------------ 532
hMATE2-B  532 GCAGGTGAGAGGCTGTGCGTCCCAGCCTCTTCCAACTCCTCAACAGGGATGGCTGAAGGG 591
hMATE2    532 ----------------------------------------------GGATGGCTGAAGGG 545

hMATE2-K  532 ------------------------------------------------------------ 532
hMATE2-B  592 GCAGGAGGAGGAGTCCCCATTCCAAACCCCGGGTTTGTCCATCCTCCATCCATCTCACTC 651
hMATE2    546 GCAGGAGGAGGAGTCCCCATTCCAAACCCCGGGTTTGTCCATCCTCCATCCATCTCACTC 605

hMATE2-K  532 ----------------------------------AAGATCACCTGGCCCCAAGTCCTCAG 557
hMATE2-B  652 ACACCTTAGCAGGGCCAGTTTTCATTTATTTCAG..................... 711
hMATE2    606 ACACCTTAGCAGGGCCAGTTTTCATTTATTTCAG..................... 665

hMATE2-K  558 TGGTGTGGTGGGCAACTGTGTCAACGGTGTGGCCAACTATGCCCTGGTTTCTGTGCTGAA 617
hMATE2-B  712 ............................................................ 771
hMATE2    666 ............................................................ 725

hMATE2-K  618 CCTGGGGGTCAG                                               629
hMATE2-B  772 ............                                               783
hMATE2    726 ............                                               737
```

*Figure 1.* Comparison of the nucleotide sequences of the exon 7 region among human kidney-specific multidrug and toxin extrusion 2 (hMATE2-K), human brain-specific multidrug and toxin extrusion 2 (hMATE2-B), and human multidrug and toxin extrusion 2 (hMATE2). Conserved nucleotides among three transporters are indicated by dots. The nucleotides are numbered starting at the first residue of the ATG putative initiation codon.

### *Cell Culture, Transfection, and Uptake Experiments*

HEK293 cells (American Type Culture Collection CRL-1573, Manassas, VA) were cultured as described previously (16,17). pcDNA3.1 (+) plasmid vector DNA that contained hMATE2-K cDNA and hMATE2-B cDNA were transfected into HEK293 cells using LipofectAMINE 2000 Reagent (Invitrogen), as described (16,17). At 48 h after the transfection, the cells were used for uptake experiments.

Cellular uptake of cationic compounds was measured with monolayer cultures of HEK293 cells that were grown on poly-D-lysine–coated 24-well plates (16,17). Typically, the cells were preincubated with 0.2 ml of incubation medium (pH 7.4) for 10 min at 37°C. The medium then was removed, and 0.2 ml of incubation medium that contained radiolabeled substrates was added. The medium was aspirated off at the end of the incubation, and the monolayers were rinsed rapidly twice with 1 ml of ice-cold incubation medium. The cells were solubilized in 0.5 ml of 0.5 N NaOH, and then the radioactivity in aliquots was determined by liquid scintillation counting. The cellular uptake of cephalexin, cefazolin, and cephradine was described previously (18). For the cellular uptake of NMN, the HEK293 cells that were transfected with the hMATE2-K cDNA were incubated with NMN for 10 min, washed twice, and scraped with 0.5 ml of incubation medium (pH 7.4). The cellular accumulation of NMN was determined by HPLC

*Table 1.* Primer sets and probes for real-time PCR and RT-PCR[a]

| Gene Name (Accession) | Positions[c] | Sequences (5′ to 3′) |
|---|---|---|
| For real-time PCR[b] | | |
| hMATE1 (AK001709) | | |
| forward primer (+) | 1240 to 1262 | ATTGGGTACTATGTGGTTGGCCT |
| reverse primer (−) | 1333 to 1311 | AGATGATGATCCCTGACCACAGA |
| TaqMan probe (+) | 1273 to 1298 | ATCGCGCTGATGTTTGCAACCACACT |
| hMATE2 (NM_152908)[d] | | |
| forward primer (+) | 1444 to 1467 | ACTGCTGCCTTTGTTGCTTATACT |
| reverse primer (−) | 1570 to 1551 | TCTCAGGCCCAGGTCTGGTT |
| TaqMan probe (−) | 1541 to 1519 | TCTGCTCTCTGCTGCTGCTGCCG |
| For RT-PCR | | |
| forward primer (+) | | ATCGTGAGCACTGTGTTCTGC |
| hMATE2-K (AB250364) | 155 to 177 | |
| hMATE2-B (AB250701) | 155 to 177 | |
| hMATE2 (NM_152908) | 155 to 177 | |
| reverse primer (−) | | TGGGAGATGATGTTGGCATA |
| hMATE2-K (AB250364) | 659 to 640 | |
| hMATE2-B (AB250701) | 813 to 794 | |
| hMATE2 (NM_152908) | 767 to 748 | |
| hGAPDH (NM_002046) | | |
| forward primer (+) | 24 to 44 | CAACGGATTTGGTCGTATTGG |
| reverse primer (−) | 836 to 816 | TGCTCAGTGTAGCCCAGGATG |

[a]hMATE1, human multidrug and toxin extrusion 1; hMATE2-B, human brain-specific multidrug and toxin extrusion 2; hMATE2-K, human kidney-specific multidrug and toxin extrusion 2; RT-PCR, reverse transcriptase–PCR.
[b]Directions of the primer sequences are denoted in the parentheses as sense (+) or antisense (−).
[c]The nucleotides are from the sequence in the GenBank Data Bank and are numbered starting at the first residue of ATG putative initiation codon.
[d]Although only the nucleotide numbers for hMATE2 are shown, the primer and probe set also reacts with hMATE2-K and hMATE2-B.

according to the method of Musfeld *et al.* (19). For manipulation of the intracellular pH, intracellular acidification was performed by pretreatment with ammonium chloride (30 mM, 20 min at 37°C, pH 7.4) (20,21). The protein content of the solubilized cells was determined using a Bio-Rad Protein Assay Kit (Bio-Rad Laboratories, Hercules, CA) with bovine γ-globulin as a standard.

### *Statistical Analyses*

Data are expressed as the mean ± SEM. Data were analyzed statistically using an unpaired *t* test. Significance was set at $P < 0.05$. In all figures, when error bars are not shown, they are smaller than the symbols.

## Results

After the sequencing of hMATE2 cDNA that was isolated from the human kidney (hMATE2-K) and human brain (hMATE2-B), it was revealed with the BLAST program that both hMATE2-K and hMATE2-B transcripts consist of 17 exons. However, a deletion of 108 bp in exon 7 of hMATE2-K and an insertion of 46 bp in exon 7 of hMATE2-B were found compared with hMATE2 (Figure 1). The open reading frame of the cloned hMATE2-K cDNA was 1698 bp, coding for a 566–amino acid protein with a calculated molecular mass of 61,012, and that of hMATE2-B was 660 bp and a 220–amino acid protein with a calculated molecular mass of 23,357. Figure 2 shows the deduced amino acid sequences of hMATE2-K and its alignment with its homologues hMATE2-B, hMATE2, hMATE1, or rat (r) MATE1, which was cloned recently in our laboratory from rat kidney with an accession no. AB248823 (22). hMATE2-K showed 82% amino acid identity with hMATE2-B, 94% with hMATE2 (12), 52% with hMATE1 (12), and 52% with rMATE1.

The hMATE1 mRNA was expressed strongly in the adrenal gland as well as in the kidney; weakly in the fetal liver, testis, skeletal muscle, liver, and uterus; and faintly in various other tissues (Figure 3A). In contrast, the obtained data showed that the transcript of the *hMATE2* gene was expressed in the kidney, because the real-time PCR condition could cross-react hMATE2-K, hMATE2-B, and hMATE2 (Figure 3A, Table 1). Although RT-PCR showed that the amplification of both products derived from hMATE2-K (505 bp) and hMATE2-B (659 bp) among 18 tissues examined, only the 505-bp band that corresponded to hMATE2-K was found in the kidney (Figure 3B). The 613-bp band that corresponded to hMATE2 was not amplified. After sequencing, the PCR product of 659 bp was confirmed to be identical to hMATE2-B.

To visualize the intrarenal distribution of hMATE2-K, we examined the immunohistochemical analysis (Figure 4). Staining with the antibodies specific for hMATE1 and hMATE2-K revealed that both transporters were localized in the brush

```
hMATE2-K     1 MDSLAQDTVALLDRGGCKFALDK----LVFKGFGTEMWTLFALSGPLFLFQVLTFRLIVST   56
hMATE2-B     1 .....E.....------.....   56
hMATE2       1 .....------.....   56
hMATE1       1 .EAPEEPAPVRG.PEATLEV.GSRC.RLSA.RE.LRA.LV.A..A..V.LMV.L.SFI.S   60
rMATE1       1 .EV.EEPAPGPG.ADAAER-.GLRR.LLS..QE.LRA.LV.A..A..A.LMM.L.SFI.S   59

hMATE2-K    57 VFCGHLGKVELASVTLAVAFVNVCGVSVGVGLSSACDTLMSQSFGSPNKKHVGVILQRGA  116
hMATE2-B    57 .....   116
hMATE2      57 .....   116
hMATE1      61 .....L..DA....I.VI..T.....F.....I..TY..Q.L.....S.  120
rMATE1      60 .....L..DA....I.VI..T.I...H.....I..TY..Q.L.....T  119

hMATE2-K   117 LVLLLCCLPCWALFLNTQHILLLFRQDPDVSRLTQDYVMIFIPGLPVIFLYNLLAKYLQN  176
hMATE2-B   117 .....   176
hMATE2     117 .....   176
hMATE1     121 .....F.....T..T....A..AT...M.QV...L.  180
rMATE1     120 .I.....F.....I..EQ.....T...V....A..AA...T.QV...L.  179

hMATE2-K   177 Q-----   177
hMATE2-B   177 .AGERLCVPASSNSSTGMAEGAGGGVPIPNPGPVHPPSISLTP-----   219
hMATE2     177 .-----GWLKGQEEESPFQTPGLSI  196
hMATE1     181 .-----   184
rMATE1     180 .-----   183

hMATE2-K   178 -----KITWPQVLSGVVGNCVNGVANYALVSVLNLGVRGSAYANIISQ  220
hMATE2-B   219 -----   219
hMATE2     197 LHPSHSHLSRASPHLFQ.....  256
hMATE1     185 -----G.VL..IVT..AA.L..AL...LPLHQ.H...I...L..L...  224
rMATE1     184 -----G.VL...IT.IAA.L..AL...LPLHQ.H...M...L..T...  223

hMATE2-K   221 FAQTVFLLLYIVLKKLRLETWAGWSSQCLQDWGPFFSLAVPSMLMICVEWWAYEIGSFLM  280
hMATE2-B   219 -----   219
hMATE2     257 .....   316
hMATE1     225 YTLALL.F...LG....QA..G...LE.....AS.LR..I.....L.M......V....S  284
rMATE1     224 ..LAI..F...LWR...HA..G...WE.....AS.LQ..I.....L.I......V....S  283

hMATE2-K   281 GLLSVVDLSAQAVIYEVATVTYMIPLGLSIGVCVRVGMALGAADTVQAKRSAVSGVLSIV  340
hMATE2-B   219 -----   219
hMATE2     317 .....   376
hMATE1     285 .I.GM.E.G..SIV..L.IIV...V.A.F.VAAS....N....G.ME..RK.STVSL.IT.  344
rMATE1     284 .I.GM.E.G..SIT..L.IIV....A.F.VAAN....N....GNID...K.SAISLIVTE  343

hMATE2-K   341 GISLVLGTLISILKNQLGHIFTNDEDVIALVSQVLPVYSVFHVFEAICCVYGGVLRGTGK  400
hMATE2-B   219 -----   219
hMATE2     377 .....   436
hMATE1     345 LFAVAFSV.LLSC.DHV.Y...T.R.I.N..A..V.I.A.S.L...LA.TS.....S.N  404
rMATE1     344 LFAVTFCV.LLGC.DLV.Y...T.W.IV....A..V.I.A.S.L...LA.TC.....N  403

hMATE2-K   401 QAFGAAVNAITYYIIGLPLGILLTPVVRMRIMGLWLGMLACVFLATAAPVAYTARLDWKL  460
hMATE2-B   219 -----   219
hMATE2     437 .....   496
hMATE1     405 .KV..I..T.G..VV...I..A.M.ATTLGV....S.III.TVFQAVC.LGFIIQ.N..K  464
rMATE1     404 .KV..I....G..V....I..S.M..AXLGVI...S.III.SVCQ.SC.LVFI...N...  463

hMATE2-K   461 AAEEAKKHSGRQQQQRAESTATRPGPEKAVLSSVATGSSPGITLTTYSRS-ECHVDFFRT  519
hMATE2-B   219 -----   219
hMATE2     497 .....   555
hMATE1     465 .CQQ.QV.ANLKVNNVPR.GNSALPQDPL-SPGCPENLEG-.LTNDVGKTG.PQS.QQMR  522
rMATE1     464 .CQQ.QV.ANLKVNVALN.A---VSQ.P.-SPVGPESHGE-.MM.DLEKKD.IQL.QQMN  518

hMATE2-K   520 PEEAHALSAPTSR-LSVKQLVIRRGAA-LGAASATLMVGLTVRILATRH----  566
hMATE2-B   219 -----   219
hMATE2     556 .....   602
hMATE1     523 Q..PLPEHPQDGAK..R....L...LLL..VFLI-.L..IL.----FYVRIQ  570
rMATE1     519 QQQ.LPVHPKD.NK..G...AL...LLP..VVLV-.VG.IL.----VYIRTE  566
```

*Figure 2.* Comparison of the deduced amino acid sequences among hMATE2-K, hMATE2-B, hMATE2, hMATE1, and rat multidrug and toxin extrusion 1 (rMATE1). The conserved residues in hMATE2-K are indicated by dots. The accession numbers for hMATE2-K, hMATE2-B, hMATE2, hMATE1, and rMATE1 are AB250364, AB250701, NM_152908, AK001709, and AB248823, respectively.

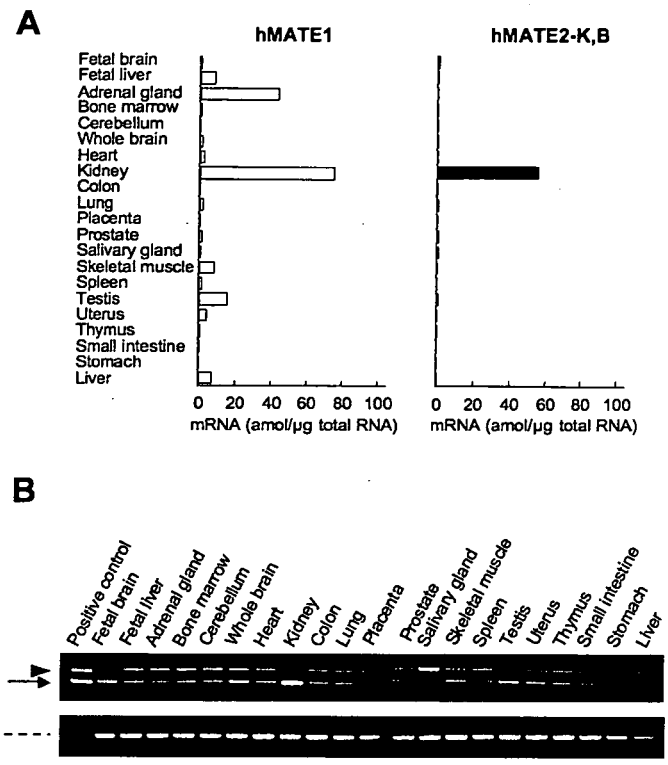


*Figure 3.* Real-time PCR for hMATE1 and hMATE2 (A), and the splice variant-specific reverse transcriptase–PCR (RT-PCR) analysis for hMATE2-K and hMATE2-B (B). (A) Total RNA isolated from various human tissues were reverse transcribed, and mRNA levels of hMATE1 and hMATE2 with their spliced variants were determined by real-time PCR with the oligonucleotides summarized in Table 1 using an ABI PRISM 7700 sequence detector. The mRNA expression level of hMATE1 and hMATE2 was calculated by the absolute standard method as described (13). As described in the legend for Table 1, the primer and probe set for hMATE2 cross-reacts with both hMATE2-K and hMATE2-B; therefore, the data are the mRNA levels of hMATE2, hMATE2-K, and hMATE2-B. Each column represents the mean of two separate experiments. (B) The RT-PCR amplification of hMATE2-K and hMATE2-B mRNA with the primer sets covering exon 7 of each gene shown in Table 1. The PCR products of 505 bp that corresponded to hMATE2-K (arrow) and 659 bp that corresponded to hMATE2-B (arrowhead) were separated by 2% agarose gel electrophoresis and visualized by ethidium bromide staining. No signal was observed of 613 bp that corresponded to hMATE2. The quality of the sample RNA also was checked by RT-PCR for glyceraldehyde-3-phosphate dehydrogenase (GAPDH) as an internal control (dotted line). The mixture of plasmid DNA coding hMATE2-K and hMATE2-B was used as a positive control for hMATE2-K and hMATE2-B and as a negative control for GAPDH.

border membranes of proximal tubules (Figure 4, A through F). Although the green signals for F-actin with phalloidin were shown in all sections, red signal was not observed in the section stained with the preimmune serum (Figure 4G). The red signals for hOCT2, which is a basolateral organic cation transporter, and the hOCTN2, which is a luminal $Na^+$/carnitine co-transporter, were confirmed in the basolateral and brush border membranes, respectively (Figure 4, H and I).

The oppositely directed $H^+$ gradient–dependent uptake of [$^{14}$C]TEA was examined in HEK293 cells that were transfected with the pcDNA3.1 (+) empty vector, hMATE2-K cDNA, and hMATE2-B cDNA. The pH gradient–dependent uptake of [$^{14}$C]TEA was stimulated in cells that were transfected with hMATE2-K cDNA but not with hMATE2-B cDNA (Figure 5A). In addition, intracellular acidification by ammonium chloride markedly stimulated the hMATE2-K–mediated uptake of [$^{14}$C]TEA, but no response was observed in hMATE2-B–transfected cells (Figure 5B). The hMATE2-K–mediated [$^{14}$C]TEA uptake was not affected by co-transfection of hMATE2-B cDNA (Figure 6). Therefore, the protein that was coded by hMATE2-B seemed to have no influence on the activity of hMATE2-K or its

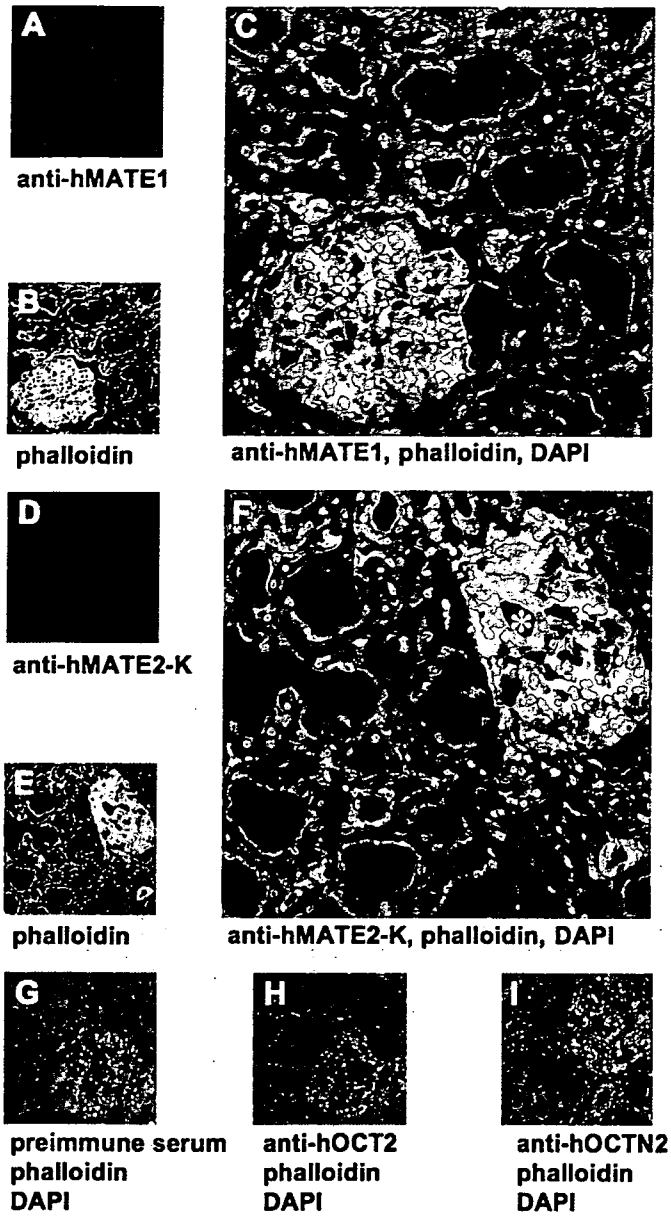


*Figure 4.* Immunofluorescence localization of hMATE1 and hMATE2-K in the human kidney. The hMATE1 (red; A), F-actin (green; B), and merged picture including the purple signals of 4′,6-diamidino-2-phenylindole (DAPI; C) were observed in the same section. The hMATE2-K (red; D), F-actin (green; E), and merged picture including DAPI (F) were in the same section. The yellow signals consist of hMATE1 or hMATE2-K and F-actin and were concentrated in the brush border membranes of proximal tubules (C and F). No positive staining for hMATE2-K (red) was observed using the preimmune serum (G). The basolateral localization of hOCT2 (H) and the apical localization of hOCTN2 (I) were confirmed with each antibody, respectively. *Glomeruli. Magnification, ×100.

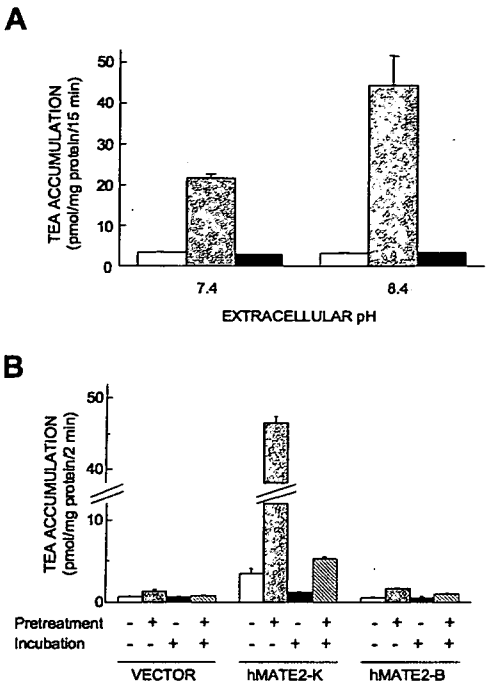


*Figure 5.* Oppositely directed $H^+$ gradient–dependent uptake of [$^{14}$C]tetraethylammonium (TEA) by hMATE2-K but not hMATE2-B in the transiently transfected HEK293 cells. (A) The pcDNA3.1(+) empty vector (□), hMATE2-K cDNA (▨), and hMATE2-B cDNA (■) were transfected into the HEK293 cells. Two days after transfection, uptake of [$^{14}$C]TEA (5 μM, 7.4 kBq/ml) was examined at the extracellular pH 7.4 or 8.4. (B) HEK293 cells that were transfected with the empty vector, hMATE2-K cDNA, and hMATE2-B cDNA were preincubated with incubation medium (pH 7.4) in the absence (□) or presence (▨) of 30 mM ammonium chloride for 20 min. Then, the preincubation medium was removed, and the cells were incubated with 5 μM [$^{14}$C]TEA (7.4 kBq/ml, pH 7.4) in the absence (■) or presence (▩) of 30 mM ammonium chloride for 2 min at 37°C. Each column represents the mean ± SE of three monolayers.

own activity as an organic cation transporter. We subsequently focused on the functional characterization of hMATE2-K. The hMATE2-K–mediated uptake of [$^{14}$C]TEA was increased in accordance with the extracellular pH between 6.0 and 9.0 (Figure 7A). Because of the apparent linearity of the time course of the hMATE2-K–mediated uptake of [$^{14}$C]TEA until 5 min (Figure 7B), the transport characteristics of hMATE2-K at 2 min were selected to examine the kinetics. The linearity of the uptakes of [$^{14}$C]metformin, [$^{3}$H]MPP, and [$^{3}$H]cimetidine also were confirmed until 5 min (data not shown). The uptake of [$^{14}$C]TEA, [$^{14}$C]metformin, [$^{3}$H]MPP, [$^{3}$H]cimetidine, and [$^{14}$C]procainamide by hMATE2-K exhibited saturable kinetics, following the Michaelis-Menten equation. The apparent Km values of TEA, metformin, MPP, cimetidine, and procainamide were estimated at 0.83 ± 0.15 mM, 1.05 ± 0.29 mM, 93.5 ± 4.9 μM, 0.37 ± 0.14 mM, and 4.10 ± 0.30 mM, respectively (Figure 8).

Next, we examined the substrate specificity of hMATE2-K. The hMATE2-K mediated the oppositely directed $H^+$ gradient–dependent transport of structurally diverse organic cations such as [$^{14}$C]TEA, [$^{3}$H]MPP, [$^{3}$H]cimetidine, [$^{14}$C]metformin, and NMN at extracellular pH 8.4 (Table 2) or at pH 7.4 after

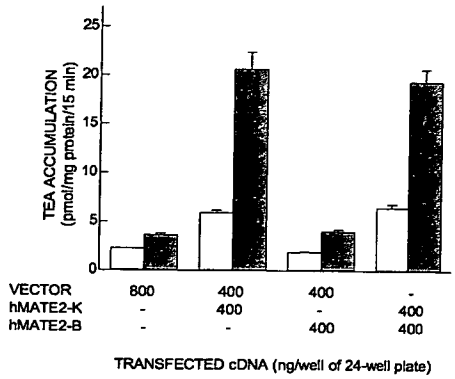


*Figure 6.* Transfection of hMATE2-B cDNA in HEK293 cells did not stimulate [$^{14}$C]TEA uptake and did not affect hMATE2-K–mediated [$^{14}$C]TEA uptake. HEK293 cells that were transfected with the empty vector (800 ng/well), hMATE2-K cDNA (400 ng/well) with the empty vector (400 ng/well), hMATE2-B cDNA (400 ng/well) with the empty vector (400 ng/well), and the combination of both hMATE2-K (400 ng/well) and hMATE2-B (400 ng/well) cDNA were incubated with 5 $\mu$M [$^{14}$C]TEA (7.4 kBq/ml) at pH 7.4 (□) or pH 8.4 (■). Each point represents the mean ± SE of three monolayers.

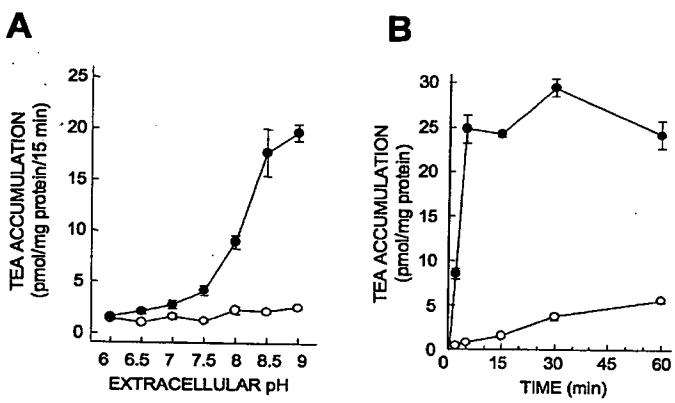


*Figure 7.* Oppositely directed $H^+$ gradient dependence (A) and time course (B) of [$^{14}$C]TEA uptake by hMATE2-K in the transiently transfected HEK293 cells. (A) HEK293 cells that were transfected with the empty vector (○) or hMATE2-K (●) were incubated for 15 min at 37°C with incubation medium of various pH that contained 5 $\mu$M of [$^{14}$C]TEA. Each point represents the mean ± SE of six monolayers by two independent experiments. (B) Time course of [$^{14}$C]TEA uptake by hMATE2-K. HEK293 cells that were transiently transfected with the empty vector (○) or hMATE2-K cDNA (●) were incubated with [$^{14}$C]TEA (5$\mu$M, 7.4kBq/ml, pH 8.4) for 15 min at 37°C. Each point represents the mean ± SE of three monolayers.

pretreatment of ammonium chloride (Table 3). The uptake of [$^{14}$C]procainamide was stimulated in hMATE2-K–expressing cells only after pretreatment of ammonium chloride (Tables 2 and 3). In addition, the uptake of [$^{14}$C]creatinine, [$^{3}$H]quinidine, [$^{3}$H]thiamine, and [$^{3}$H]verapamil was increased in hMATE2-K–expressing cells with treatment of ammonium chloride. However, the anionic compounds *p*-aminohippuric acid, dipeptide

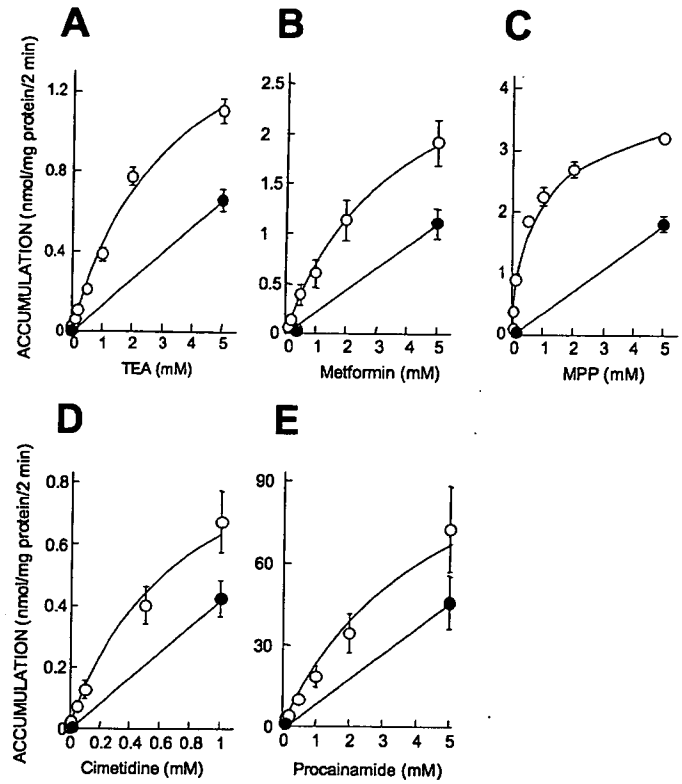


*Figure 8.* Concentration dependence of hMATE2-K–mediated uptake of [$^{14}$C]TEA (A), [$^{14}$C]metformin (B), [$^{3}$H]1-methyl-4-phenylpyridinium (MPP; C), [$^{3}$H]cimetidine (D), and [$^{14}$C]procainamide (E). HEK293 cells that were transfected with hMATE2-K cDNA were incubated with various concentrations of [$^{14}$C]TEA (pH 8.4; A) or [$^{14}$C]metformin (pH 8.4; B). For the kinetic analyses of [$^{3}$H]MPP (C), [$^{3}$H]cimetidine (D), and [$^{14}$C]procainamide (E) at pH 7.4, ammonium chloride (30 mM, pH 7.4, 20 min) was pretreated to generate the condition of intracellular acidification. Uptake experiments were performed in the absence (○) or presence of each unlabeled substrate at 10 mM (●) for 2 min at 37°C. Each point represents the mean ± SE of four independent experiments.

glycylsarcosine, and $\beta$-lactam antibiotics were not transported by hMATE2-K.

## Discussion

In this study, we cloned an alternatively spliced variant of hMATE2 from the human kidney, hMATE2-K (Figures 1 and 2). The hMATE2 that originated from the human brain was not expressed in the kidney (Figure 3). In addition, another variant was cloned from the human brain, hMATE2-B, but original hMATE2 was not cloned from either kidney or brain. hMATE2-B cDNA contains a 154-bp insertion in exon 7 of hMATE2-K and a 46-bp insertion in exon 7 of hMATE2. The hMATE2-B has only 220 amino acids by the 46-bp insertion in exon 7 of MATE2; therefore, the truncated product of the gene, hMATE2-B, seems to lack the transport activity (Figures 5 and 6). Although an RT-PCR band that corresponded to hMATE2-B but not hMATE2 was ubiquitously found, the expression level of the gene was markedly low in consideration of the result of real-time PCR (Figure 3). Consid-

*Table 2.* Uptake of various organic ions in the HEK293 cells that expressed hMATE2-K at extracellular pH 8.4[a]

| Compounds | Vector | hMATE2-K |
|---|---|---|
| Uptake (μl/mg protein per 15 min) | | |
| [$^{14}$C]TEA | 0.48 ± 0.00 | 2.65 ± 0.04[b] |
| [$^{3}$H]MPP | 2.44 ± 0.61 | 5.56 ± 0.12[c] |
| [$^{3}$H]cimetidine | 1.19 ± 0.05 | 2.08 ± 0.06[b] |
| [$^{14}$C]metformin | 0.85 ± 0.05 | 2.48 ± 0.08[b] |
| [$^{14}$C]creatinine | 2.60 ± 0.05 | 2.68 ± 0.11 |
| [$^{14}$C]guanidine | 11.0 ± 0.02 | 8.93 ± 0.21[c] |
| [$^{14}$C]procainamide | 12.1 ± 0.98 | 12.0 ± 0.21 |
| [$^{14}$C]choline | 105 ± 0.69 | 91.5 ± 0.18[b] |
| [$^{3}$H]quinidine | 137 ± 2.56 | 148 ± 6.16 |
| [$^{3}$H]quinine | 170 ± 7.83 | 229 ± 3.99[b] |
| [$^{3}$H]thiamine | 13.8 ± 0.46 | 11.5 ± 0.52[c] |
| [$^{3}$H]carnitine | 10.9 ± 0.67 | 10.3 ± 0.70 |
| [$^{14}$C]nicotine | 8.16 ± 0.91 | 9.94 ± 0.18 |
| [$^{14}$C]captopril | 0.45 ± 0.02 | 0.63 ± 0.05[c] |
| [$^{3}$H]verapamil | 11.6 ± 0.23 | 16.0 ± 3.58 |
| [$^{14}$C]levofloxacin | 7.60 ± 1.47 | 6.66 ± 0.17 |
| [$^{3}$H]tetracycline | 5.86 ± 0.16 | 6.14 ± 0.01 |
| [$^{14}$C]*p*-aminohippuric acid | 4.90 ± 0.16 | 4.54 ± 0.13 |
| [$^{3}$H]glycylsarcosine | 0.70 ± 0.07 | 0.59 ± 0.07 |
| Uptake (μl/mg protein per 10 min) | | |
| NMN | 0.47 ± 0.04 | 1.63 ± 0.65[c] |
| cephalexin | 0.13 ± 0.02 | 0.14 ± 0.05 |
| cefazolin | 0.17 ± 0.03 | 0.10 ± 0.02 |
| cephradine | 0.20 ± 0.03 | 0.20 ± 0.02 |

[a]HEK293 cells cultured in a 24-well plate were transfected with the empty vector or hMATE2-K cDNA and incubated for 15 min with incubation medium at pH 8.4 that contained the 19 radiolabeled compounds indicated. After incubation, the radioactivities of solubilized cells were determined. HEK293 cells cultured in a 12-well plate and expressed hMATE2-K were incubated for 10 min with incubation medium at pH 8.4 that contained 1 mM unlabeled $N^1$-methylnicotinamide (NMN) or β -lactam antibiotics such as cephalexin, cefazolin, and cephradine. After incubation, the amounts of each compound extracted from cells were determined by HPLC. Uptake was expressed as clearance, which was obtained from the net uptake value divided by each substrate concentration in the medium. Data represent the mean ± SEM for three monolayers. MPP, 1-methyl-4-phenylpyridinium acetate; TEA, tetraethylammonium.

[b]$P < 0.01$, [c]$P < 0.05$ significantly different from vector-transfected cells.

ering the 108- and 154-bp deletions in hMATE2-K compared with hMATE2 and hMATE2-B, respectively, the splicing site differed between the kidney and other tissues.

Examination of the tissue distribution clearly indicated that hMATE2-K was a kidney-specific type $H^+$/organic cation antiporter, whereas hMATE1 mRNA was found in several tissues (Figure 3A). Although hMATE1 mRNA was strongly expressed in the kidney, it also was preferentially expressed in the adrenal gland, liver, skeletal muscle, and testis, corresponding to the report by Otsuka *et al.* (12). Comparing promoter sequences between hMATE1 and hMATE2-K should help to reveal the molecular mechanisms behind the kidney-specific expression of hMATE2-K as well as other renal organic ion transporters hOCT2 (SLC22A2), hOAT1 (SLC22A6), and hOAT3 (SLC22A8) (10). Immunohistochemical examinations clearly demonstrated the apical localization of hMATE2-K protein as well as hMATE1 protein in the proximal tubules (Figure 4, A through F) (12). Considering the functional characteristics and the membrane localization, hMATE2-K was indicated to mediate tubular secretion of cationic compounds at the brush border membranes. These results suggest that some cationic drugs that are preferentially recognized by hMATE2-K are eliminated predominantly through urine *via* tubular secretion, whereas those that are recognized by hMATE1 are excreted into both bile and urine. Therefore, the substrate specificities between these two transporters should be clarified to understand kidney/liver selectivity in the elimination route of the organic cations.

Although the uptake of procainamide was not observed at pH 8.4, it was stimulated by the pretreatment with ammonium chloride (Tables 2 and 3). These results suggest that hMATE2-K requires a strong driving force, a counteracting $H^+$ gradient across the plasma membrane, for the transport of procainamide. Stoichiometric determination would clarify the coupling ratio between the substrate and $H^+$ ion or the mass charge of the substrate in combination with the $H^+$ ion. In addition, further transport studies should be carried out to clarify the precise requirement(s) of the chemical structure(s) to understand the substrate specificity of hMATE2-K.

*Table 3.* Uptake of various organic ions in HEK293 cells that expressed hMATE2-K at extracellular pH 7.4 after pretreatment of ammonium chloride[a]

| Compounds | Vector | hMATE2-K |
|---|---|---|
| Uptake (μl/mg protein per 2 min) | | |
| [$^{14}$C]TEA | 0.36 ± 0.04 | 7.71 ± 0.10[b] |
| [$^{3}$H]MPP | 3.87 ± 0.07 | 19.5 ± 0.31[b] |
| [$^{3}$H]cimetidine | 1.00 ± 0.12 | 9.24 ± 0.06[b] |
| [$^{14}$C]metformin | 0.56 ± 0.01 | 6.68 ± 0.42[b] |
| [$^{14}$C]creatinine | 0.58 ± 0.05 | 0.93 ± 0.07[c] |
| [$^{14}$C]guanidine | 3.10 ± 0.18 | 3.71 ± 0.05[c] |
| [$^{14}$C]procainamide | 14.9 ± 0.11 | 18.5 ± 0.67[b] |
| [$^{14}$C]choline | 7.64 ± 0.14 | 8.08 ± 0.21 |
| [$^{3}$H]quinidine | 108 ± 2.01 | 126 ± 2.21[b] |
| [$^{3}$H]quinine | 109 ± 0.60 | 124 ± 5.10[c] |
| [$^{3}$H]thiamine | 5.98 ± 0.06 | 12.4 ± 5.10[b] |
| [$^{3}$H]carnitine | 12.16 ± 0.08 | 12.7 ± 0.26 |
| [$^{14}$C]nicotine | 7.05 ± 0.32 | 7.97 ± 0.20 |
| [$^{14}$C]captopril | 0.32 ± 0.01 | 0.27 ± 0.02 |
| [$^{3}$H]verapamil | 24.09 ± 1.54 | 30.5 ± 0.05[c] |
| [$^{14}$C]levofloxacin | 9.29 ± 0.19 | 10.1 ± 0.83 |
| [$^{3}$H]tetracycline | 3.46 ± 0.16 | 4.06 ± 0.19 |
| [$^{14}$C]*p*-aminohippuric acid | 1.14 ± 0.03 | 1.33 ± 0.12 |
| [$^{3}$H]glycylsarcosine | 0.26 ± 0.01 | 0.33 ± 0.03 |
| Uptake (μl/mg protein per 10 min) | | |
| NMN | 0.51 ± 0.03 | 2.54 ± 0.36[b] |
| cephalexin | 0.13 ± 0.01 | 0.16 ± 0.03 |
| cefazolin | 0.14 ± 0.05 | 0.07 ± 0.01 |
| cephradine | 0.27 ± 0.04 | 0.30 ± 0.03 |

[a]HEK293 cells cultured in a 24-well plate for the uptake examination of radiolabeled compounds or cultured in a 12-well plate for unlabeled compounds were transfected with the empty vector or hMATE2-K cDNA and incubated for 20 min with incubation medium that contained 30 mM ammonium chloride. After washing, 2- or 10-min uptake measurements at extracellular pH 7.4 were carried out for radiolabeled or unlabeled compounds as described in the legend for Table 2, respectively. Data represent the mean ± SEM for three monolayers.
[b]$P < 0.01$, [c]$P < 0.05$ significantly different from vector-transfected cells.

In this study, an antihyperglycemic agent, metformin, was demonstrated for the first time to be a good substrate for hMATE2-K (Figure 8B, Tables 2 and 3). There is no information available about the $H^+$ gradient–dependent transport of metformin in renal brush border membrane vesicles. Actually, approximately 70% of metformin in the circulation was eliminated in urine mainly *via* tubular secretion, and when co-administered, cimetidine decreased the renal clearance of metformin (23,24). Recently, we demonstrated that metformin is a superior substrate for renal OCT2 rather than hepatic OCT1 (17,25). Renal distribution of metformin immediately after intravenous administration was almost 23-fold higher than the plasma concentration in the rats (1.29 μg/ml in plasma *versus* 29.8 μg/g in kidney at 3 min after intravenous administration) (17). This background and our results strongly suggest that renal hMATE2-K plays a key role in the tubular secretion of metformin after basolateral accumulation by renal hOCT2.

## Conclusion

An active variant, hMATE2-K, and a longer variant, hMATE2-B, were cloned and characterized. It is indicated that hMATE2-K is the first kidney-specific $H^+$/organic cation antiporter to mediate the tubular secretion of a wide range of cationic compounds across the brush border membranes in the proximal tubules. The physiologic roles of hMATE2-B and hMATE2, including the expressional characteristics of these genes, still are unclear. Further studies should be performed to elucidate the physiologic and pharmacologic significance of hMATE2-K as well as hMATE1 in the renal handling of ionic drugs.

## Acknowledgments

This work was supported in part by a grant-in-aid for Research on Advanced Medical Technology from the Ministry of Health, Labor and Welfare of Japan; by the Japan Health Science Foundation "Research on Health Sciences Focusing on Drug Innovation"; by a grant-in-aid for

Scientific Research from the Ministry of Education, Science, Culture and Sports of Japan; and by the 21st Century COE program "Knowledge Information Infrastructure for Genome Science." A.Y. was supported as a Research Assistant by the 21st Century COE program "Knowledge Information Infrastructure for Genome Science."

## References

1. Ullrich KJ: Renal transporters for organic anions and organic cations. Structural requirements for substrates. *J Membr Biol* 158: 95–107, 1997
2. Inui K, Okuda M: Cellular and molecular mechanisms of renal tubular secretion of organic anions and cations. *Clin Exp Nephrol* 2: 100–108, 1998
3. Takano M, Inui K, Okano T, Saito H, Hori R: Carrier-mediated transport systems of tetraethylammonium in rat renal brush-border and basolateral membrane vesicles. *Biochim Biophys Acta* 773: 113–124, 1984
4. Inui K, Takano M, Okano T, Hori R: H+ gradient-dependent transport of aminocephalosporins in rat renal brush border membrane vesicles: Role of H+/organic cation antiport system. *J Pharmacol Exp Ther* 233: 181–185, 1985
5. Hori R, Maegawa H, Okano T, Takano M, Inui K: Effect of sulfhydryl reagents on tetraethylammonium transport in rat renal brush border membranes. *J Pharmacol Exp Ther* 241: 1010–1016, 1987
6. Maegawa H, Kato M, Inui K, Hori R: pH sensitivity of H+/organic cation antiport system in rat renal brush-border membranes. *J Biol Chem* 263: 11150–11154, 1988
7. Katsura T, Maegawa H, Tomita Y, Takano M, Inui K, Hori R: Trans-stimulation effect on H+-organic cation antiport system in rat renal brush-border membranes. *Am J Physiol* 261: F774–F778, 1991
8. Grundemann D, Gorboulev V, Gambaryan S, Veyhl M, Koepsell H: Drug excretion mediated by a new prototype of polyspecific transporter. *Nature* 372: 549–552, 1994
9. Gorboulev V, Ulzheimer JC, Akhoundova A, Ulzheimer-Teuber I, Karbach U, Quester S, Baumann C, Lang F, Busch AE, Koepsell H: Cloning and characterization of two human polyspecific organic cation transporters. *DNA Cell Biol* 16: 871–881, 1997
10. Inui K, Masuda S, Saito H: Cellular and molecular aspects of drug transport in the kidney. *Kidney Int* 58: 944–958, 2000
11. Koepsell H, Endou H: The SLC22 drug transporter family. *Pflugers Arch* 447: 666–676, 2004
12. Otsuka M, Matsumoto T, Morimoto R, Arioka S, Omote H, Moriyama Y: A human transporter protein that mediates the final excretion step for toxic organic cations. *Proc Natl Acad Sci U S A* 102: 17923–17928, 2005
13. Motohashi H, Sakurai Y, Saito H, Masuda S, Urakami Y, Goto M, Fukatsu A, Ogawa O, Inui K: Gene expression levels and immunolocalization of organic ion transporters in the human kidney. *J Am Soc Nephrol* 13: 866–874, 2002
14. Ji L, Masuda S, Saito H, Inui K: Down-regulation of rat organic cation transporter rOCT2 by 5/6 nephrectomy. *Kidney Int* 62: 514–524, 2002
15. Masuda S, Saito H, Nonoguchi H, Tomita K, Inui K: mRNA distribution and membrane localization of the OAT-K1 organic anion transporter in rat renal tubules. *FEBS Lett* 407: 127–131, 1997
16. Urakami Y, Akazawa M, Saito H, Okuda M, Inui K: cDNA cloning, functional characterization, and tissue distribution of an alternatively spliced variant of organic cation transporter hOCT2 predominantly expressed in the human kidney. *J Am Soc Nephrol* 13: 1703–1710, 2002
17. Kimura N, Masuda S, Tanihara Y, Ueo H, Okuda M, Katsura T, Inui K: Metformin is a superior substrate for renal organic cation transporter OCT2 rather than hepatic OCT1. *Drug Metab Pharmacokinet* 20: 379–386, 2005
18. Ueo H, Motohashi H, Katsura T, Inui K: Human organic anion transporter hOAT3 is a potent transporter of cephalosporin antibiotics, in comparison with hOAT1. *Biochem Pharmacol* 70: 1104–1113, 2005
19. Musfeld C, Biollaz J, Belaz N, Kesselring UW, Decosterd LA: Validation of an HPLC method for the determination of urinary and plasma levels of N1-methylnicotinamide, an endogenous marker of renal cationic transport and plasma flow. *J Pharm Biomed Anal* 24: 391–404, 2001
20. Jans AW, Amsler K, Griewel B, Kinne RK: Regulation of intracellular pH in LLC-PK1 cells studied using 31P-NMR spectroscopy. *Biochim Biophys Acta* 927: 203–212, 1987
21. Lang K, Wagner C, Haddad G, Burnekova O, Geibel J: Intracellular pH activates membrane-bound Na(+)/H(+) exchanger and vacuolar H(+)-ATPase in human embryonic kidney (HEK) cells. *Cell Physiol Biochem* 13: 257–262, 2003
22. Terada T, Masuda S, Asaka J, Tsuda M, Katsura T, Inui K: Molecular cloning, functional characterization and tissue distribution of rat H+/organic cation antiporter MATE1. *Pharm Res* 2006, in press
23. Sirtori CR, Franceschini G, Galli-Kienle M, Cighetti G, Galli G, Bondioli A, Conti F: Disposition of metformin (N,N-dimethylbiguanide) in man. *Clin Pharmacol Ther* 24: 683–693, 1978
24. Somogyi A, Stockley C, Keal J, Rolan P, Bochner F: Reduction of metformin renal tubular secretion by cimetidine in man. *Br J Clin Pharmacol* 23: 545–551, 1987
25. Kimura N, Okuda M, Inui K: Metformin transport by renal basolateral organic cation transporter hOCT2. *Pharm Res* 22: 255–259, 2005

*Pharmaceutical Research, Vol. 23, No. 8, August 2006 (© 2006)*
DOI: 10.1007/s11095-006-9016-3

*Short Communication*

# Molecular Cloning, Functional Characterization and Tissue Distribution of Rat H$^+$/Organic Cation Antiporter MATE1

**Tomohiro Terada,[1] Satohiro Masuda,[1] Jun-ichi Asaka,[1] Masahiro Tsuda,[1] Toshiya Katsura,[1] and Ken-ichi Inui[1,2]**

*Received February 18, 2006; accepted March 21, 2006*

***Purpose.*** Transport characteristics and tissue distribution of the rat H$^+$/organic cation antiporter MATE1 (multidrug and toxin extrusion 1) were examined.
***Methods.*** Rat MATE1 cDNA was isolated by polymerase chain reaction (PCR) cloning. Transport characteristics of rat MATE1 were assessed by HEK293 cells transiently expressing rat MATE1. The mRNA expression of rat MATE1 was examined by Northern blot and real-time PCR analyses.
***Results.*** The uptake of a prototypical organic cation tetraethylammonium (TEA) by MATE1-expressing cells was concentration-dependent, and showed the greatest value at pH 8.4 and the lowest at pH 6.0–6.5. Intracellular acidification induced by ammonium chloride resulted in a marked stimulation of TEA uptake. MATE1 transported not only organic cations such as cimetidine and metformin but also the zwitterionic compound cephalexin. MATE1 mRNA was expressed abundantly in the kidney and placenta, slightly in the spleen, but not expressed in the liver. Real-time PCR analysis of microdissected nephron segments showed that MATE1 was primarily expressed in the proximal convoluted and straight tubules.
***Conclusions.*** These findings indicate that MATE1 is expressed in the renal proximal tubules and can mediate the transport of various organic cations and cephalexin using an oppositely directed H$^+$ gradient.

**KEY WORDS:** H$^+$/organic cation antiporter; kidney; MATE1; renal secretion.

## INTRODUCTION

The secretion of drugs and xenobiotics is an important physiological function of the renal proximal tubules. Functional studies using isolated membrane vesicles and cultured renal epithelial cells have suggested that the renal tubular secretion of cationic substances involves concerted actions of two distinct classes of organic cation transporters: one facilitated by the transmembrane potential difference in the basolateral membrane and the other driven by the transmembrane H$^+$ gradient (H$^+$/organic cation antiporter) in the brush-border membrane (1,2). The membrane-potential dependent organic cation transporters (OCT1-3, SLC22A1-3) have been identified and well characterized (3–5), but the molecular nature of the H$^+$/organic cation antiporter has not been elucidated for a long time.

Recently, based on in silico homology screening, human and mouse orthologues of the multidrug and toxin extrusion (MATE) family, which confers multidrug resistance to bacteria, have been identified (6). The tissue distribution, membrane localization and transport characteristics of human MATE1 suggested that this transporter is similar to transporters of the renal H$^+$-coupled organic cation export system (6). However, the precise substrate specificity based on direct uptake measurements and expression profiles of wide-ranging tissues for MATE1 have not been evaluated. So far, we have characterized the functional properties of H$^+$/organic cation antiporters in the rat kidney (7–12). In the present study, we isolated rat MATE1 cDNA and investigated the transport characteristics and tissue and intrarenal distribution of this transporter.

## MATERIALS AND METHODS

### Materials

Cephalexin (Shionogi, Osaka, Japan) and cefazolin (Fujisawa Pharmaceutical Co., Osaka, Japan) were donated by the respective suppliers. [$^{14}$C]Tetraethylammonium bromide (TEA) (2.035 GBq/mmol), [$^{14}$C]creatinine (2.035 GBq/mmol) and [$^{14}$C]procainamide (2.035 GBq/mmol) were obtained from American Radiolabeled Chemicals Inc (St. Louis, MO). [$^{14}$C]Metformin (962 MBq/mmol) and [$^{14}$C]guanidine hydrochloride (1.961 Gbq/mmol) were purchased from Moravek Biochemicals Inc (Brea, CA). [$^3$H]1-Methyl-4-phenylpyridinium acetate (MPP) (2.7 TBq/mmol) and [$^{14}$C]*p*-aminohippurate (PAH) (1.9 GBq/mmol) were from PerkinElmer Life Analytical Sciences (Boston, MA). [*N*-Methyl-$^3$H]Cimetidine (451 GBq/mmol) was obtained from

[1] Department of Pharmacy, Kyoto University Hospital, Sakyo-ku, Kyoto 606-8507, Japan.
[2] To whom correspondence should be addressed. (e-mail: inui@kuhp.kyoto-u.ac.jp)

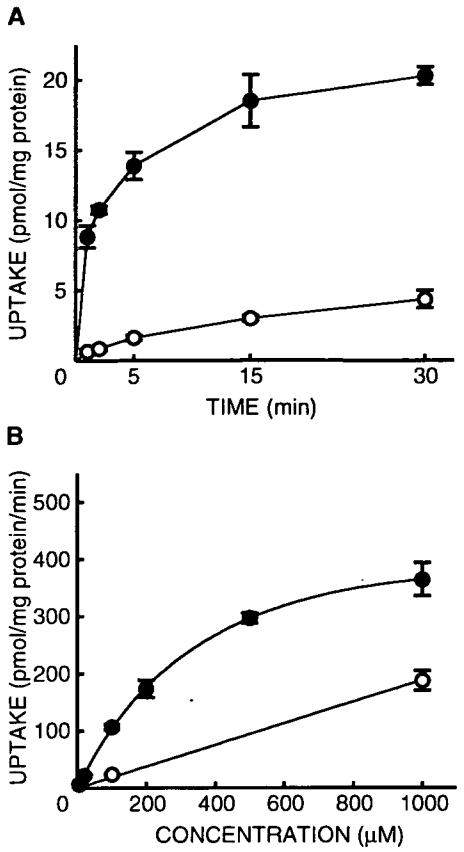


**Fig. 1.** Transport of [$^{14}$C]TEA by rat MATE1. **A** Time course of [$^{14}$C]TEA uptake by HEK293 cells transiently expressing rat MATE1. HEK293 cells transfected with vector alone (pcDNA3.1) (○) or MATE1 cDNA (●) were incubated with 5 μM of [$^{14}$C]TEA (pH 8.4) at 37°C. Each point represents the mean ± S.E. for three monolayers. **B** Concentration-dependence of [$^{14}$C]TEA uptake by HEK293 cells transiently expressing rat MATE1. HEK293 cells transfected with rat MATE1 cDNA were incubated with various concentrations of [$^{14}$C]TEA (pH 8.4) in the absence (●) or presence of 5 mM TEA (○) for 1 min at 37°C. This figure shows representative data of three separate experiments. Each point represents the mean ± S.E. for three monolayers.

Amersham Biosciences (Uppsala, Sweden). $N^1$-Methylnicotinamide (NMN) was purchased from Sigma (St. Louis, MO). All other chemicals used were of the highest purity available.

### cDNA Cloning of Rat MATE1

Rat MATE1 cDNA was isolated from Marathon-Ready rat kidney cDNA (Clontech, Palo Alto, CA) using specific primers designed based on sequence information of the NCBI reference sequence NM_001014118 and human MATE1 (6). The rat MATE1 cDNA was cloned using the following primers: forward 5′-CACATGGAGGTCTTG GAGGAGCCTGCGCCG-3′ and reverse 5′-CACAGACT GAGGAGCACCTGCATTGCTGG-3′. The PCR product was subcloned into the expression vector pcDNA3.1 (+) (Invitrogen, Carlsbad, CA), and sequenced by a multicapillary DNA sequencer RISA384 system (Shimadzu, Kyoto, Japan). The nucleotide sequence for the open reading frame of rat MATE1 was identical to the NCBI reference sequence NM_001014118 except for G1608T, which substituted Tyr for Asp at position 529 (variant 2). This transporter had the same ability to transport [$^{14}$C]TEA and [$^{14}$C]metformin as the reference type of MATE1 (variant 1). The nucleotide sequences reported here have been submitted to the DDBJ/EMBL/GenBank Data Bank with Accession No. AB248823 (variant 1) and No. AB248824 (variant 2).

### Cell Culture and Transfection

HEK293 cells (American Type Culture Collection CRL-1573) were cultured as described previously (13–15). pcDNA 3.1 (+) containing cDNA encoding rat MATE1 was transfected into HEK293 cells using LipofectAMINE 2000 Reagent (Invitrogen) according to the manufacturer's instructions. At 48 h after the transfection, the cells were used for uptake experiments.

### Uptake Experiments in HEK293 Cells

The cellular uptake of various radiolabeled compounds was measured by monolayers grown on poly-D-lysine-coated 24-well plates as described previously (13–15). Typically, the cells were preincubated with 0.2 ml of incubation medium (pH 7.4) for 10 min at 37°C. The medium was then removed, and 0.2 ml of incubation medium (pH 8.4) containing a radiolabeled compound such as [$^{14}$C]TEA was added. After an appropriate period of incubation, the medium was aspirated, and the monolayers were washed twice with 1 ml of ice-cold incubation medium. The cells were solubilized in 0.5 ml of 0.5 N NaOH, and then the radioactivity in aliquots was determined by liquid scintillation counting. Furthermore, the cellular uptake of cephalosporin antibiotics was measured as described previously (15). For cellular uptake of NMN, HEK293 cells expressing rat MATE1 were incubated with NMN for 1 h, washed two times, and scraped with 0.5 ml of incubation medium (pH 7.4). The accumulation of NMN was determined according to the method of Musfeld *et al.* (16). The conditions for high-performance liquid chromatography (HPLC) were as follows: column, Zorbax ODS column 4.6 mm inside diameter × 250 mm (Du Pont, Wilmington, DE, USA); mobile phase, 5 mM sodium heptanesulfonate containing 0.5% triethylamine (pH 3.2):acetonitrile = 78:22; flow rate, 1.0 ml/min; excitation and emission wavelengths, 366 and 418 nm, respectively; temperature, 40°C.

### Northern Blot Analysis and Real-time PCR for Various Tissues and Microdissected Nephron Segments

The preparation of total RNA and Northern blot analysis under the high-stringency conditions were performed as described previously (17). Total RNA from various rat tissues was purchased from BioChain (Hayward, CA), and reverse transcribed (18). Isolation of total RNA from microdissected nephron segments and reverse transcription (RT) were previously reported (19,20). Using these RT products, real-time PCR was carried out (18). The primer-probe set used for rat MATE1 was as follows: forward primer, 5′-GGG CATCGCTGCTAACCTT-3′ (bp 567–585); reverse primer, 5′-CCCCAAGATGTAGCTGATGGA-3′ (bp 654–634); fluorescence probe, 5′-(6-Fam) TCAACGCCCTGGCCAA

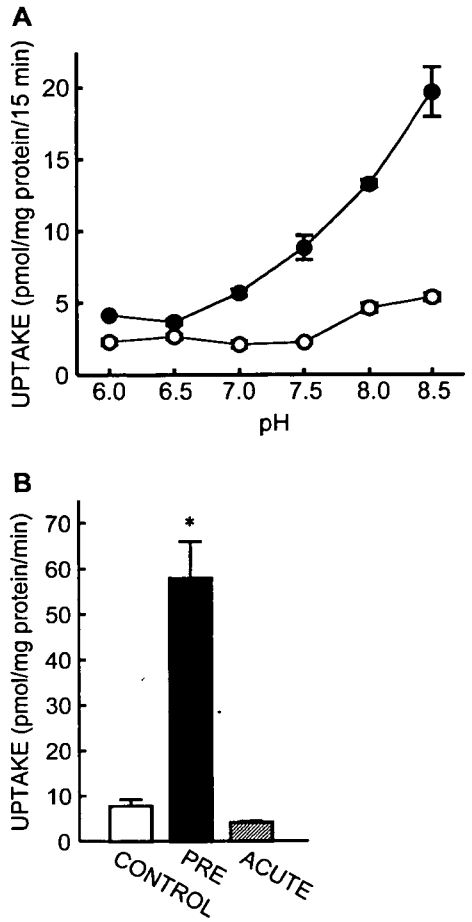


**Fig. 2.** Effect of pH on the transport of [$^{14}$C]TEA by rat MATE1. **A** Effect of extracellular pH on [$^{14}$C]TEA uptake by HEK293 cells transiently expressing rat MATE1. HEK293 cells transfected with vector alone (pcDNA3.1) (○) or rat MATE1 cDNA (●) were incubated with 5 μM of [$^{14}$C]TEA (pH 8.4) for 15 min at 37°C. **B** Effect of intracellular pH on [$^{14}$C]TEA uptake by HEK293 cells transiently expressing rat MATE1. HEK293 cells transfected with MATE1 cDNA were preincubated with incubation medium (pH 7.4) in the absence (CONTROL and ACUTE) or presence (PRE) of 30 mM ammonium chloride for 20 min (21). Then, the preincubation medium was removed, and the cells were incubated with 5 μM of [$^{14}$C]TEA (pH 8.4) in the absence (CONTROL and PRE) or presence (ACUTE) of 30 mM ammonium chloride for 1 min at 37°C. Each point represents the mean ± S.E. for three monolayers. *$P < 0.05$, significantly different from CONTROL.

CTATCTGTTT (Tamra)(phosphate)-3′ (bp 587–612). The primer-probe sets used for rat OCT1 and OCT2 were predeveloped TaqMan Assay Reagents (Applied Biosystems, Foster, CA). Glyceraldehyde-3-phosphate dehydrogenase (GAPDH) mRNA was also measured as an internal control with GAPDH Control Reagent (Applied Biosystems).

### Statistical Analyses

Data were analyzed statistically using a non-paired *t* test (Fig. 3B) or a one-way analysis of variance followed by Sheffé's test (Fig. 2B). *P* values of less than 0.05 were considered significant. In all figures, when error bars are not shown, they are smaller than the symbol.

## RESULTS

We cloned rat MATE1 cDNA from rat kidney by PCR cloning. Rat MATE1 showed 79% amino acid identity with human MATE1, 91% with mouse MATE1, 48% with human MATE2 and 57% with mouse MATE2 (6). When rat MATE1 was expressed in HEK293 cells, a time- and concentration-dependent uptake of [$^{14}$C]TEA was observed (Fig. 1). The uptake by MATE1 exhibited saturable kinetics, following the Michaelis–Menten equation. The apparent Km value of the uptake was calculated at 570 ± 64 μM.

Figure 2 shows the effects of changes in extra- and intracellular pH on [$^{14}$C]TEA uptake by MATE1. When the extracellular pH was changed from 6.0 to 8.4, the uptake was greatest at pH 8.4 and lowest at pH 6.0–6.5. Intracellular pH

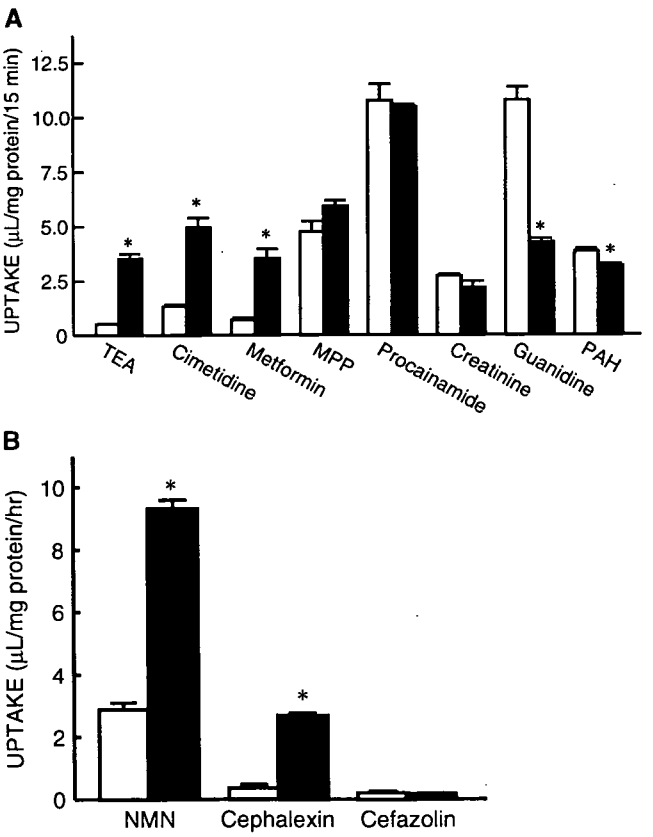


**Fig. 3.** Uptake of various compounds by rat MATE1. **A** Uptake of various radiolabeled compounds by HEK293 cells transiently expressing rat MATE1. HEK293 cells transfected with vector alone (pcDNA3.1) (*open column*) or MATE1 cDNA (*closed column*) were incubated with [$^{14}$C]TEA (5 μM), [$^{3}$H]cimetidine (23 nM), [$^{3}$H]MPP (3.8 nM), [$^{14}$C]metformin (10 μM), [$^{14}$C]creatinine (5 μM), [$^{14}$C]guanidine (5 μM), [$^{14}$C]procainamide (5 μM) or [$^{14}$C]PAH (5 μM) for 15 min at 37°C. After the incubation, the radioactivity of solubilized cells was determined. **B** Uptake of NMN, cephalexin and cefazolin by HEK293 cells transiently expressing rat MATE1. HEK293 cells transfected with vector alone (pcDNA3.1) (*open column*) or MATE1 cDNA (*closed column*) were incubated with each compound (1 mM) for 1 h at 37°C. After the incubation, amounts of each compound extracted from cells were determined by HPLC. Uptake was expressed as clearance, which was obtained by dividing the net uptake value by the concentration of each substrate in the medium. Each column represents the mean ± S.E. for three monolayers.

was manipulated by treating the cells with ammonium chloride according to a previous report (21). When ammonium chloride is added to a preincubation medium and then removed (pretreatment), the intracellular pH falls. However, the exposure of cells to ammonium chloride (acute treatment) causes a rapid alkalization of the intracellular pH. As shown in Fig. 2B, intracellular acidification through pretreatment resulted in a marked stimulation of [$^{14}$C]TEA uptake, whereas the uptake was reduced by acute treatment.

We then examined the substrate specificity of MATE1. As shown in Fig. 3, MATE1 mediated the transport of several organic cations with different chemical structures such as [$^{14}$C]TEA, [$^{3}$H]cimetidine, [$^{14}$C]metformin, and NMN. In addition, MATE1 transported the zwitterionic cephalosporin cephalexin, which was demonstrated to be a substrate for the rat $H^+$/organic cation antiporter in the membrane vesicle studies (8). In contrast, MATE1 did not transport cationic compounds such as [$^{3}$H]MPP, [$^{14}$C]procainamide, [$^{14}$C]creatinine and [$^{14}$C]guanidine, the anionic compound [$^{14}$C]PAH, or the anionic cephalosporin cefazolin.

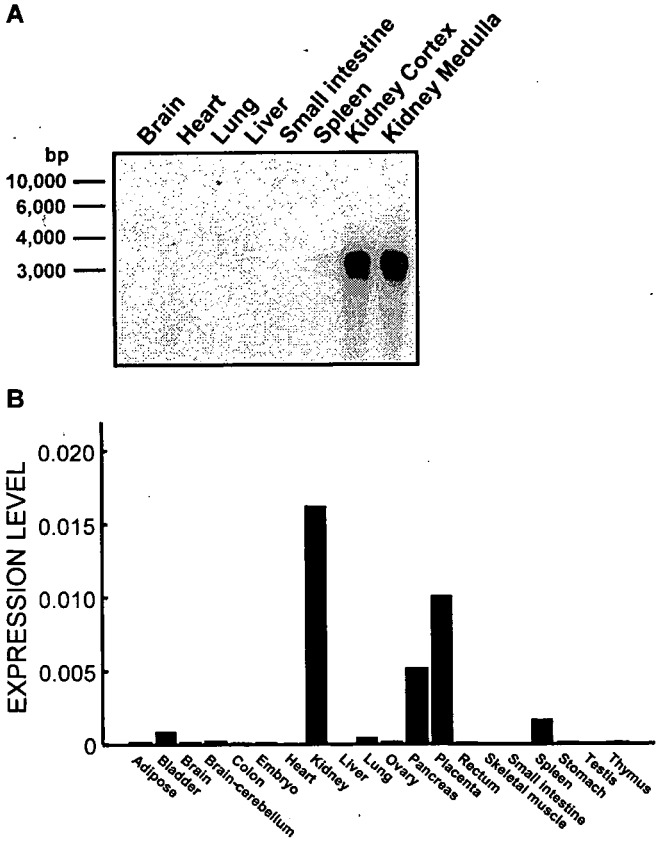


**Fig. 4.** Tissue distribution of rat MATE1. **A** Northern blot analysis of MATE1 mRNA in rat tissues. Total RNA (30 μg) from the indicated tissues was electrophoresed, blotted, and hybridized with a specific probe for rat MATE1 under high stringency conditions. **B** Real-time PCR for MATE1 mRNA in rat tissues. RNA from various rat tissues was reverse-transcribed, and rat MATE1 and GAPDH mRNA levels were determined by real-time PCR using an ABI PRISM 7700 sequence detector. The mRNA expression level of rat MATE1 is represented as a ratio of that of GAPDH in each tissue. Each column represents the mean for two separate experiments.

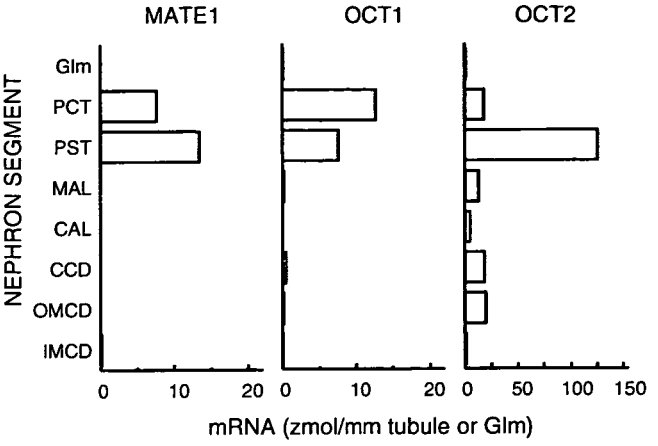


**Fig. 5.** Distribution of rat MATE1, OCT1 and OCT2 mRNAs along the microdissected renal nephron segments. Each PCR was performed using part of RT reaction derived from 10 glomeruli and 5 mm of renal tubules. The mRNA expression levels of rat MATE1, OCT1 and OCT2 were determined by real-time PCR using an ABI PRISM 7700 sequence detector. Each column represents the mean for two separate experiments. *Glm* glomerulus, *PCT* proximal convoluted tubule, *PST* proximal straight tubule, *MAL* medullary thick ascending limb, *CAL* cortical thick ascending limb, *CCD* cortical collecting duct, *OMCD* outer medullary collecting duct, *IMCD* inner medullary collecting duct.

Finally, tissue distribution of rat MATE1 mRNA was examined. High-stringency Northern blot analysis revealed that a transcript (about 3.5 KB) of rat MATE1 was strongly expressed in the kidney cortex and medulla, and faintly in the spleen (Fig. 4A). No positive signal was detected in other tissues, including the brain, small intestine and liver (Fig. 4A). The results of real-time PCR analyses using RNA from various rat tissues were consistent with the results of the Northern blot analysis. MATE1 mRNA was highly expressed in the kidney and placenta, and slightly expressed in the pancreas, spleen, bladder and lung (Fig. 4B).

To determine the distribution of rat MATE1 mRNA along the nephron segments, real-time PCR analysis using microdissected nephron segments was performed, as comparing with those of rat OCT1 and OCT2 mRNA. As shown in Fig. 5, rat MATE1 mRNA was primarily expressed in the proximal convoluted tubule (PCT) and proximal straight tubule (PST). The expression of rat OCT1 mRNA was also found in the PCT and PST. Rat OCT2 mRNA was highly expressed in PST with about 10 fold higher expression level as compared with that of rat MATE1 or OCT1 mRNA, and significant expression was also detected in other segments such as PCT, outer medullary collecting duct (OMCD) and cortical collecting duct (CCD). Distribution of rat OCT1 and OCT2 mRNA was corresponded to a previous report (20).

## DISCUSSION

Using renal brush-border membrane vesicles, the transport of TEA (7,22,23), aminocephalosporins (8), cimetidine (9,24,25), NMN (26) and procainamide (27) was examined, and demonstrated to be actively driven by an outwardly directed $H^+$ gradient via the $H^+$/organic cation antiport

system. By using a renal epithelial cell line LLC-$PK_1$, the apical transport of TEA (28,29) and procainamide (30) was demonstrated to be mediated by the $H^+$/organic cation antiport system. In the present study, we found that most of these organic compounds were transported by rat MATE1. However, procainamide was not transported, although rat OCT1 and OCT2 can transport procainamide (unpublished data). As the transport of procainamide via the $H^+$/organic cation antiport system was demonstrated in rabbit renal brush-border membrane vesicles (27) and porcine LLC-$PK_1$ cells (30), a species difference may be responsible for this discrepancy. Using human renal brush-border membrane vesicles, Chun *et al.* (31) found that transport of guanidine was stimulated by $H^+$ gradient, and that the mechanism involved was distinct from that for the transport of TEA and NMN. Although species differences should be taken into consideration, the present findings that guanidine was not transported by rat MATE1 may support the membrane vesicle study (31). Taken together, these findings suggest that other MATE isoforms reported in humans (6) may be involved in the transport of procainamide and guanidine in the renal brush-border membrane. Further studies are needed to clarify the molecular mechanisms responsible for the diversity of organic cation transport in the renal brush-border membrane.

Otsuka *et al.* (6) reported that [$^{14}$C]TEA transport by human MATE1 was inhibited by MPP, but not by NMN. In the present study, rat MATE1 was able to transport NMN, but not MPP. These findings suggest that human and rat MATE1 have different properties of substrate recognition for these compounds. Experimental conditions such as inhibition studies (6) and our uptake studies may also explain the different findings.

Rat MATE1 mRNA is highly expressed in the kidney, especially in the proximal tubules, and placenta, but not in the liver. In contrast, human MATE1 is preferentially expressed in the kidney and liver, but not in the placenta (6), indicating a clear species difference in the distribution of MATE1 mRNA between human and rat. Previous studies using vesicles prepared from rat sinusoidal membranes (32) and from human term placenta (33) revealed the presence of a $H^+$/organic cation antiport system in these tissues. Detailed functional characterization suggested that the system in the liver and placenta differs from the renal system (32,33), and MATE1 mRNA expression in rat and human tissues supports these assumptions. Other molecules than MATE1 may be responsible for the $H^+$/organic cation antiport in the rat liver and human placenta.

The transport of organic cations such as TEA and cimetidine in the renal brush-border membrane was mediated by $H^+$/organic cation antiport system energized by a transmembrane $H^+$ gradient (1,2). Since the luminal pH is more acidic than the intracellular pH in the proximal tubules (34), due to an $Na^+/H^+$ antiporter and/or ATP-driven $H^+$-pump, it is reasonable to assume that the inward $H^+$ gradient (luminal pH<intracellular pH) can drive the secretion of organic cations *in vivo*. Human MATE1 exhibited pH-dependent transport of TEA in cellular uptake and efflux studies (6), but these analyses are not enough to prove the $H^+$/TEA antiport mechanism. It is possible that pH-dependent transport of TEA may be due to the modulation of transport activity caused by changes in extracellular pH. In the present study, we found that intracellular acidification by ammonium chloride pretreatment resulted in the marked stimulation of [$^{14}$C]TEA uptake by MATE1, suggesting that outwardly directed $H^+$ gradient serves as a driving force for MATE1 (Fig. 2B).

In conclusion, rat MATE1 is abundantly expressed in the renal proximal tubules, and can accept various compounds including organic cations and zwitterionic cephalosporin as substrates. Changes in extra- and intracellular pH suggested that an oppositely directed $H^+$ gradient works as a driving force for MATE1. Although further studies are needed to elucidate the physiological and pharmacokinetic roles of this transporter, the present findings can provide important information about the renal tubular secretion of organic cations.

## ACKNOWLEDGMENTS

This work was supported in part by the 21st Century COE program "Knowledge Information Infrastructure for Genome Science," a Grant-in-Aid for Scientific Research from the Ministry of Education, Culture, Sports, Science and Technology of Japan, and a Grant-in-Aid for Research on Advanced Medical Technology from the Ministry of Health, Labor and Welfare of Japan. J.A. is supported as a Research Assistant by the 21st Century COE program "Knowledge Information Infrastructure for Genome Science."

## REFERENCES

1. J. B. Pritchard and D. S. Miller. Mechanisms mediating renal secretion of organic anions and cations. *Physiol. Rev.* **73**:765–796 (1993).
2. K. Inui and M. Okuda. Cellular and molecular mechanisms of renal tubular secretion of organic anions and cations. *Clin. Exp. Nephrol.* **2**:100–108 (1998).
3. K. Inui, S. Masuda, and H. Saito. Cellular and molecular aspects of drug transport in the kidney. *Kidney Int.* **58**:944–958 (2000).
4. B. C. Burckhardt and G. Burckhardt. Transport of organic anions across the basolateral membrane of proximal tubule cells. *Rev. Physiol. Biochem. Pharmacol.* **146**:95–158 (2003).
5. H. Koepsell and H. Endou. The SLC22 drug transporter family. *Pflügers Arch.* **447**:666–676 (2004).
6. M. Otsuka, T. Matsumoto, R. Morimoto, S. Arioka, H. Omote, and Y. Moriyama. A human transporter protein that mediates the final excretion step for toxic organic cations. *Proc. Natl. Acad. Sci. USA* **102**:17923–17928 (2005).
7. M. Takano, K. Inui, T. Okano, H. Saito, and R. Hori. Carrier-mediated transport systems of tetraethylammonium in rat renal brush-border and basolateral membrane vesicles. *Biochim. Biophys. Acta* **773**:113–124 (1984).
8. K. Inui, M. Takano, T. Okano, and R. Hori. $H^+$ gradient-dependent transport of aminocephalosporins in rat renal brush border membrane vesicles: role of $H^+$/organic cation antiport system. *J. Pharmacol. Exp. Ther.* **233**:181–185 (1985).
9. M. Takano, K. Inui, T. Okano, and R. Hori. Cimetidine transport in rat renal brush border and basolateral membrane vesicles. *Life Sci.* **37**:1579–1585 (1985).
10. R. Hori, H. Maegawa, T. Okano, M. Takano, and K. Inui. Effect of sulfhydryl reagents on tetraethylammonium transport in rat renal brush border membranes. *J. Pharmacol. Exp. Ther.* **241**: 1010–1016 (1987).
11. H. Maegawa, M. Kato, K. Inui, and R. Hori. pH sensitivity of $H^+$/organic cation antiport system in rat renal brush-border membranes. *J. Biol. Chem.* **263**:11150–11154 (1988).